Penetrating the air-liquid interface is the key to colonization and Wrinkly Spreader fitness

Robyn Jerdan
Anna Kuśmierska
Marija Petric
Andrew J. Spiers

Microbiology Second Revised Manuscript

Penetrating the air-liquid interface is the key to colonization and Wrinkly Spreader fitness

Robyn Jerdan[1], Anna Kuśmierska[1,2], Marija Petric[1] & Andrew J. Spiers[1]

Affiliations 1 School of Applied Sciences, Abertay University, Dundee DD1 1HG, United Kingdom.

2 Department of Industrial Microbiology and Biotechnology, Faculty of Biology and Environmental Protection, University of Łódź, Łódź, Poland.

Corresponding Author A.J. Spiers. E-mail: a.spiers@abertay.ac.uk

Key Words Ecological opportunity, experimental evolution, Goldilocks zone, microcosms, *Pseudomonas fluorescens,* surface tension.

Abbreviations SAA, Surface-active agent; SBW25, *Pseudomonas fluorescens* SBW25; ST, Surface tension; WS, Wrinkly Spreader.

ABSTRACT

In radiating populations of *Pseudomonas fluorescens* SBW25, adaptive Wrinkly Spreader (WS) mutants are able to gain access to the air-liquid (A-L) interface of static liquid microcosms and achieve a significant competitive fitness advantage over other non-biofilm–forming competitors. Aerotaxis and flagella-based swimming allows SBW25 cells to move into the high-O_2 region located at the top of the liquid column and maintain their position by countering the effects of random cell diffusion, convection and disturbance (i.e. physical displacement). However, wild-type cells showed significantly lower levels of enrichment in this region compared to the archetypal Wrinkly Spreader, indicating that WS cells employ an additional mechanism to transfer to the A-L interface where displacement is no longer an issue and a biofilm can develop at the top of the liquid column. Preliminary experiments suggest that this might be achieved through the expression of an as-yet unidentified surface active agent which is weakly associated with WS cells and alters liquid surface tension as determined by quantitative tensiometry. The effect of physical displacement on the colonization of the high-O_2 region and A-L interface was reduced through addition of agar or polyethylene glycol to increase liquid viscosity, and under these conditions, WS competitive fitness was significantly reduced. These observations suggest that the ability to transfer to the A-L interface from the high–O_2 region and remain there without further expenditure of energy (through for example, the deployment of flagella) is a key evolutionary innovation of the Wrinkly Spreader, as it allows subsequent biofilm development and significant population increase, thereby affording these adaptive mutants with a competitive fitness advantage over non-biofilm–forming competitors located within in the liquid column.

INTRODUCTION

Adaptive radiation, a central element in evolution [1,2] can be investigated by experimental evolution studies using fast growing bacterial populations in continuous chemostats or serially-transferred cultures, where abiotic and biotic factors are readily manipulated to alter selective pressures, and where simple mutations and phenotype changes (key innovations) lead to fitness advantages in adaptive lineages [3-6]. Although perhaps arcane, experimental evolution studies are relevant to medical and veterinary microbiology, agriculture, food and bio-technology, because populations radiate and communities undergo succession, and emerging adaptive lineages may have significantly-altered colonization, competitive, resistance or functional characteristics.

One such experimental evolution system uses populations of *Pseudomonas fluorescens* SBW25 (hereafter SBW25) [7,8] incubated statically in microcosms (small vials containing nutrient-rich liquid growth medium) where O_2 availability is the growth-limiting resource [9,10]. In these, early wild-type colonists establish an O_2 gradient dividing the liquid column into a shallow high-O_2 (top) region immediately below the air-liquid (A-L) interface (the 'Goldilocks zone' where growth is optimal [11,12]) above a deeper low-O_2 region where growth is limited [10]. It is important to distinguish between the A-L interface, a nanometer–deep molecular layer at the surface which is difficult to break [13], and the high-O_2 region immediately below in which cells are able to move freely but are subject to random cell diffusion (Brownian motion), convection currents and disturbance (collectively referred to here as physical displacement). The Wrinkly Spreaders (WS), a class of adaptive mutants, are able to produce a robust and well-attached biofilm at the A-L interface [9,14] (sometimes referred to as a pellicle, but see [15]) with a competitive fitness advantage over the non-biofilm–forming ancestral (wild-type) SBW25 [12,16] (see **Supplementary Figure S1** for images of WS biofilms and the high–O_2 region *in situ*). Under some circumstances, wild-type SBW25 is also able to produce a fragile and poorly attached Viscous Mass (VM) biofilm at the A-L interface which nonetheless also provides a fitness advantage over non-biofilm–forming competitors [17].

Mutations targeting diguanylate cyclases or their cognate repressors [18-22] leading to higher levels of c-*di*-GMP are responsible for the WS phenotype. The increase in c-*di*-GMP levels results in the over-expression of partially-acetylated cellulose, which is the main extracellular polysaccharide (EPS) matrix material, and poly-N-acetylglucosamine (PNAG) attachment factor which was originally thought to be a curli or pili-like fibre in early work [12,14,16,21,23,24]. Significantly, this and other bacterial experimental evolution studies have demonstrated that mutations affecting regulatory networks are capable of bringing about substantial shifts in phenotype with significant improvements in fitness, and that not all evolutionary innovation is the result of the acquisition of new function by gene duplication and divergence, *de novo* mutation of noncoding sequences or horizontal (lateral) gene transfer [25-27].

Although the underlying molecular biology and evolutionary ecology of the Wrinkly Spreader is well-understood, we have recently questioned why these adaptive mutants employ biofilm–formation to colonise the A-L interface when O_2-directed flagella-mediated swimming (i.e. aerotaxis [28]) should be sufficient to access the O_2-rich region and maintain position by countering physical displacement. SBW25 is capable of swimming [24,29-34] and is chemotaxic [31], however, aerotaxis has not been reported formally although an aerotaxis sensor receptor is annotated in the genome [35]. WS mutants are not the only strains that benefits from accessing the top layer of liquid columns, as A-L interface biofilm–formation is commonplace among pseudomonads and other bacteria (e.g. [36-40]) suggesting that this ability provides substantial benefits in a range of environments where O_2 gradients prevail. In particular, colonization of the surface microlayer of marine and freshwater habitats allows access to stratified organic compounds including lipids, polysaccharides and proteins [41-44]. Similar benefits are likely to be available in partially-saturated soil-pore networks and transient puddles on plants and other surfaces [45,46].

In this work, we demonstrate that although SBW25 is aerotaxic and swimming can overcome the effects of physical displacement in static microcosms, wild-type cells are not maintained effectively in the high-O_2 region. In contrast, it appears that WS cells are able to transfer more efficiently from the high-O_2 region and penetrate the A-L interface where they can remain in place without further energy expenditure. We then further demonstrate the value of this transfer in fitness terms by modifying the viscosity of the liquid column which reduces the impact of physical displacement and thus lowers the relative value of biofilm–formation by the Wrinkly Spreader.

METHODS

Bacteria and culture conditions

The bacterial strains used in this study included wild-type *Pseudomonas fluorescens* SBW25 [7,8], the chemotaxic-deficient but swimming *cheA*$^-$ mutant (SBW25 *cheA::aph* [31]), the non-swimming flagella-deficient *fleQ*$^-$ mutant (SBW25 Δ*fleQ* [34]) and the archetypal biofilm–forming Wrinkly Spreader (WS; SBW25 *wspF* A901C [14,18]). A further 25 independent WS isolates were recovered from experimental microcosms in this work (see below). Bacteria were cultured at 20 °C in King's B (KB) medium (20 g Proteose Peptone No. 3 (BD Biosciences, UK), 10 g glycerol, 5 g K_2HPO_4, 1.5 g $MgSO_4$ per litre [47]) and M9 minimal salts [48] and maintained at -80 °C as 15 % (w/v) glycerol stocks. Standard KB plates contained 1.5 % (w/v) agar and soft-agar used for swimming and aerotaxis assays contained 0.1x normal levels of KB nutrients and 0.3% (w/v) agar. Over-night shaken cultures in KB were used as a source of inoculum for experiments and all assays were performed at 20°C. Culture densities were determined by optical density (OD_{600}) measurements, and these and other absorbance (A) measurements were made using a Spectronic Helios Epsilon spectrophotometer (Thermo Fisher Scientific, UK) with 10 mm optical-path disposable plastic cuvettes.

Experimental microcosms

Standard microcosms were 30 ml Universal glass vials containing 6 ml KB (producing a liquid column of ~12 mm) with 20 µM 2,2-dipyridyl (Sigma, UK) and 0.1 µM Tiron (1,2-dihydroxybenzene-3,5-disulfonic acid) (Fisher Chemicals, UK) (KB-DP/T) to chelate iron and reduce unwanted VM biofilm–formation by wild-type SBW25 [17]. Microcosms were incubated with loose lids statically or with shaking at 150 rpm using a Stuart S150 orbital incubator (Bibby Scientific Ltd, UK). Methylene blue, which is decolourised under O_2-depleted conditions, was added to 0.0005% (w/v) to visualise the high-O_2 region [49]. Modified microcosms used to test the effects of increased viscosity contained a range of additives and after preliminary tests, low, medium and high concentrations (0.01%, 0.05% and 0.1% (w/v)) of agar (Technical No. 3, Oxoid, UK) and low, medium and high concentrations (1%, 2.5% and 5% (w/v)) of polyethylene glycol (PEG 10,000, Sigma) were used for further experiments. Microcosms were brought to a brief boil using a microwave oven to melt any gels and then equilibrated at 55 °C before inocula were added, gently mixed and allowed to cool before incubation. The toxic effect of low, medium and high concentrations of agar and PEG on growth in KB-DP/T was assessed in shaken microcosms. Replicate microcosms (n = 3) were inoculated with 10 µl aliquots of over-night SBW25 cultures and incubated for 24 h with shaking before growth was determined by OD_{600} measurements. Growth on PEG as the sole nutrient was measured in a similar way using shaken microcosms containing low, medium and high concentrations of PEG in M9 minimal salts.

Aerotaxis

The aerotaxic behaviour of wild-type SBW25 cells was visualised in soft-agar test tubes in which cells mid-way down the agar column could migrate towards the bottom or open-end of the test tube over 48 hr (see **Supplementary Information S1** for further details). The behaviour of wild-type, *fleQ*$^-$ and WS cells near the A-L interface was also examined by microscopy. Samples of an over-night culture were placed onto replica microscope slides (n = 5) and three sides of the coverslip were sealed with Entellan (Merk, UK) to form a chamber. These were exposed to nitrogen gas at 20 °C for 30 minutes and visualised using Leica DMR microscope and a Sony EXWAVE HD 3CCD colour camera. The slides were then left under normal O_2 conditions (air) for a further 30 minutes to re-equilibrate and further images were taken. Cells numbers were determined within a standard polygon placed along the A-L interface in each pair of images, avoiding out-of-focus cells attached to the glass surfaces, and aerotaxis behaviour is reported as the O_2 / N_2 cell number ratio.

Cell behaviours and biofilm assays

Flagella-mediated swimming motility of wild-type, *cheA*$^-$, *fleQ*$^-$ and WS cells were assessed at 20 °C using soft-agar plates with replicate inoculations using over-night cultures (n = 8 – 16) [24]. KB medium and cell densities were determined by replicate (n = 5) weight and volume measurements of 50 ml KB and over-night wild-type cultures. Sedimentation of *fleQ*$^-$ cells was observed in microcosms inoculated with re-suspended cells obtained from over-night cultures after 24 h. Similarly, microcosms inoculated with wild-type cells at high concentrations were visually assessed for downward-moving plumes characteristic of bioconvection currents. Cell distributions and enrichment are reported as relative OD_{600} determined by measuring 1 ml aliquots taken from undisturbed or mixed replicate microcosms (n = 3 – 5) inoculated with 100 µl of over-night wild-type, *fleQ*$^-$ and WS cultures and incubated for 1 – 24 h before sampling. In these assays it should be noted that the measured cell densities are the result of both cell migration and growth over the period of incubation and not simply due to motility. Sampling positions and reference measurements also varied depending on the difficulty of taking samples without disturbing the rest of the microcosm for each assay, and the cell distribution ratios are always reported such that higher values indicate greater enrichment of cells in the upper regions of the microcosm. The combined biofilm assay [37] was used to determine biofilm strength (grams), attachment levels (Crystal violet staining, A_{570}) and total microcosm growth (OD_{600} following vigorous mixing) of the independent WS isolates recovered from experimental microcosms in replicate microcosms (*n* = 8) after 3 days.

Experimental evolution and competitive fitness

The evolution of Wrinkly Spreaders from developing wild-type populations was determined over 6 days using replicate standard and modified microcosms (*n* = 5) [50]. These were inoculated with 10 µl aliquots of over-night shaken wild-type cultures and incubated statically for 1, 3 and 6 days before vigorous mixing and diluted samples spread on KB plates to determine total viable numbers and the proportion (%) of WS cells. Randomly-chosen independent WS isolates (one from each replicate microcosm, *n* = 25 in total) were recovered from the Day 3 plates for further analysis (Day 3 is an arbitrary choice which originates from the isolation of the archetypal WS from a three day-old population [14]). WS competitive fitness (W) was determined relative to wild-type cells in static and shaken microcosms [50]. Microcosms (*n* = 5) were inoculated with 60 µl aliquots of a 1:1 mixture of over-night wild-type and WS cultures and incubated statically or with shaking for 3 days before assay. Competitive fitness was calculated as *ln* [final WS numbers / initial WS numbers] / *ln* [final wild-type numbers / initial wild-type numbers] where colony counts on KB plates were used to determine cell numbers per microcosm [51] (W > 1 indicates that the WS has an advantage compared to the wild-type). In such three day assays, WS competition is largely with wild-type cells and WS – WS competition limited [12,16]; W > 1 is expected in static microcosms and W ≤ 1 in shaken microcosms where biofilms cannot form.

Viscosity and liquid surface tension measurements

The viscosity (mPa s) of standard KB-DP/T and modified media containing agar and PEG were determined at 20 °C using a DHR2 rheometer fitted with a 40 mm 1° cone and plate by the Centre for Industrial Rheology (Hampshire, UK). Briefly, following a 60 s equilibration, replicate (*n* = 3) samples were exposed to a shear rate down-sweep, from 1,000 s^{-1} to 1 s^{-1}, logarithmically scaled with 8 points per decade of shear rate, and shear applied for 30 s at each rate with viscosity calculated over the final 5 s of each step. Final viscosities for comparative purposes were determined for a shear rate of 100 s^{-1}. The viscosity of KB-DP/T with low concentrations of agar and PEG were interpolated assuming a simple linear relationship. The liquid surface tension (ST) (mN m^{-1}) of replicate re-suspended wild-type and WS cell samples, cultures and cell-free culture supernatants (n = 4) (from 18 h shaken cultures) was determined at 20 °C with a K100 Mk2 tensiometer (Krüss, Germany) using an SV23 AI/PTFE conical sample vessel and platinum testing rod, following established methods [17,52]. Under the conditions used here, the ST of deionised water and sterile KB-DP/T was 73.1 ± 0.2 and 43.6 ± 1.6 mN m^{-1}, respectively.

Statistical analyses

Experiments were undertaken with replicates (n) and means with standard errors (SE) are reported where appropriate. Data were investigated using JMP 12 statistical software (SAS Institute Inc., USA) and checked for quality before analysis. Means were compared by T-test and ANOVA models with *post-hoc* Tukey-Kramer HSD (α = 0.05) and Dunnett's Method with a control (α = 0.05) comparisons between means. Outlier analyses was undertaken by the inspection of residuals and the goodness-of-fit of Normal distributions fitted to the residuals examined by Shapiro-Wilk W tests. Where necessary, non-parametric Kruskall-Wallis (Rank Sums) tests and comparisons with a control using the Dunn Method for Joint Ranking were undertaken. A General linear modelling (GLM) approach was used to model biofilm strength, attachment and total growth as response variables with WS isolate, origin and experimental replicate as effects. However, in order to avoid singularity problems, it was necessary to nest isolate within origin (i.e. isolate[origin]) and the final models included isolate[origin], origin and replicate as effects. Outlier analyses was undertaken and residuals shown to be Normaly distributed (Shapiro-Wilk W, P > 0.05). All models were robust (model summary statistics: r^2 = 0.4 – 0.8; ANOVA, P < 0.05) and replicate was not significant in any model (P < 0.05). LSMeans Differences Tukey HSD tests were used to investigate differences between means ($\alpha = 0.05$). Means were further examined by Principal component analysis (PCA) with the Bartlett test used to confirm the significance of the two principle axes.

RESULTS

Aerotaxis allows partial localisation of cells to the high-O_2 region

The ability to migrate along an increasing O_2 gradient is an essential behaviour which would allow wild-type SBW25 cells to access the high-O_2 region of static microcosms. SBW25 is capable of flagella-mediated swimming [24,29-34], and our preliminary experiments demonstrated that wild-type cells migrated towards the open end of soft-agar test tubes in a classic display of bacterial aerotaxis (**Figure 1a**). In order to confirm this behaviour, we quantified the distribution of wild-type and WS cells in microscope slide chambers which were first first purged with N_2 to remove O_2 and then allowed to re-equilibrate with air (**Figure 1b & c**). In these assays, we used the flagella-deficient, non-motile *fleQ*$^-$ mutant cells as an aerotaxis-negative control (i.e. these cells cannot swim up an O_2 gradient) which produced an O_2 / N_2 cell number ratio of 1.1 ± 0.1 that was not significantly greater than one (T-test, $P = 0.33$) as expected, having confirmed that *fleQ*$^-$ cells were non-motile using soft-agar swimming assays (see **Supplementary Information S2** and **Figure S2** for further details). In comparison, relatively more wild-type and WS cells localised close to the A-L interface at the edge of the chamber after re-equilibration with air which demonstrates that these cells are aerotaxic (Wild-type cells, 1.6 ± 0.1, WS cells, 1.4 ± 0.1 O_2 / N_2 cell number ratio; ratios are significantly different to one, T-tests, $P > 0.05$). Furthermore, as wild-type and WS cells showed a net movement towards to the A-L interface, these assays also demonstrate that under the conditions tested here cells using aerotaxis are able to overcome the effects of random cell diffusion which would otherwise result in the slow movement of cells away from the interface.

The relative strength of aerotaxis compared to random cell diffusion should be reflected in a diffusion (effective) coefficient for motile bacteria (D_B) which is substantially greater than the corresponding diffusivity of a similarly-sized but inert sphere (D_S). D_B is given by [μ_{max}^2 τ] / 3 where μ_{max} is the maximum swimming speed and τ the mean time between tumbles or the duration of runs [53,54]. We calculated D_B for SBW25 as 2,400 – 4,200 μm^2 s^{-1} by taking τ as 1.2 s and μ_{max} as 77.6 – 102 µm s^{-1} determined by single-cell microscopy of swimmimg wild-type SBW25 cells [33]. We estimate D_S as 2.9 – 38 x 10^{-8} μm^2 s^{-1} using the mean SBW25 cell diameter of 0.9 µm and cell body length plus flagella of 11.5 µm from [33] as the spherical diameters (see **Supplementary Information S3** for further details). As $D_B >>> D_S$ as expected, we conclude that continuous aerotaxis would be sufficient to localise cells to the high-O_2 region by countering the effects of random cell diffusion.

In order to determine the significance of swimming motility to access the high-O_2 region of static microcosms, we investigated the ability of cells to move from concentrated cell pellets placed at the bottom of microcosms into the liquid column, and from a random mixture in the liquid column up to the high-O_2 region and A-L interface. We monitored cell distributions (relative OD_{600}) over 24 h and under the conditions used here, O_2 gradients develop within 3 h of inoculation [10] and these can be visualised using Methylene blue after 24 h (**Supplementary Figure S1b**). In a preliminary comparison, motile wild-type cells were found to rapidly access the liquid column from cell pellets within 12 h (**Supplementary Figure S3**), whereas no significant enrichment of the liquid column by non-aerotaxic *fleQ*$^-$ cells occurred after 24 h (Wild-type cells, 0.92 ± 0.04, *cf. fleQ*$^-$ cells, 0.16 ± 0.01 Top / Bottom OD_{600} ratio; T-test, $P < 0.0001$).

We then tested the ability of wild-type and WS cells to move from the liquid column up into the high-O_2 region and A-L interface, again using *fleQ*$^-$ cells as an aerotaxis-negative control. After inoculating microcosms with cells, we vigorously mixed them to produce a uniform cell distribution throughout the liquid column before incubation and sampling to determine cell distributions after 24 h. In these assays, wild-type cells were significantly enriched in the top 2 mm of the liquid column (corresponding to the top 1 ml) after 24 h (TK-HSD, $\alpha = 0.05$) (**Figure 2**), whereas *fleQ*$^-$ cells showed no enrichment in this region (TK-HSD, $\alpha = 0.05$) but accumulated at the bottom where a light sedimentation was observed (our measurements confirmed that the density of wild-type cells was 1.3-fold greater than that of the growth medium; K-W, $P = 0.01$). In comparison, WS cells, also capable of swimming motility [24] (see **Supplementary Information S2** and **Figure S2** for further details), showed even greater levels of enrichment than wild-type cells (~1.5-fold higher; WS cells, 1.78 ± 0.03 *cf.* Wild-type cells, 1.19 ± 0.04 Top / Mixed control OD_{600} ratio; T-test, $P = 0.008$) where the WS biofilm was included as part of the top 1 ml sample (**Figure 2c**). As FleQ is a transcriptional regulator of cellulose production in SBW25 [55], we do not use the *fleQ*$^-$ mutant in any further assays where pleitropic effects may confound our understanding of how WS cells associate with the A-L interface and form a biofilm.

Bioconvection currents are known to transport bacterial cells, O_2 and nutrients, etc. down from the high-O_2 region of liquid columns and are thought to be generated by cycles of swimming and rest of aerotaxic bacteria which have cell densities greater than the bulk liquid [56]. We were not able to confirm the presence of bioconvection currents by visual observation, as has recently been reported for wild-type SBW25 using larger microcosms and a custom-made detection system [57]. Critically, we note that, if bioconvection currents exist under the conditions tested here, they do not prevent the localisation of cells to the high-O_2 region (i.e. downward plumes are countered by the constant upward aerotaxis of displaced cells) though it might partially explain why enrichment levels in this region are not higher than observed (i.e. cells are constantly removed from the high–O_2 region by these currents).

These results clearly demonstrate that SBW25 cells can partially localise at the top of the liquid column in static microcosms through O_2-directed flagella-mediated swimming, but aerotaxis alone cannot explain the higher levels of WS cell enrichment in the high–O_2 region compared to wild-type cells. This difference suggests that WS cells have an additional capability allowing a more successful or efficient colonization of this region and the A-L interface.

Penetrating the A-L interface

Organic molecules collecting at the A-L interface of a liquid column are expected to alter the A-L interfacial tension (more commonly referred to as surface tension, ST). Experiments investigating the association of bacterial cells to thin organic layers over-laying water have also demonstrated a decrease in ST [58] (interfacial storage G' (elasticity) and loss modulus G" (viscosity) are similarly affected [59]). We therefore predict that, if WS cells were more capable of associating with the A-L interface than wild-type cells, then this should be manifested by a lower ST. A significant difference in ST was observed between wild-type and WS cultures (Wild-type culture, 32.9 ± 0.4 *cf.* WS culture, 31.0 ± 0.4 mN m^{-1}; T-test, $P = 0.02$), but not between cell-free culture supernatants which would include secreted compounds (T-test, $P = 0.18$) or between vigorously washed and re-suspended cells which would have lost weakly-associated surface material (T-test, $P = 0.16$) (**Figure 3**). Given the very small differences observed between mean measurements, we re-analysed these data using a non-parametric approach which is less sensitive to small sample sizes and found the same outcomes (K-W; cultures, $P = 0.03$; supernatants, $P = 0.14$; cells, $P = 0.29$).

We interpret these results to suggest that the Wrinkly Spreader may be producing a surface-active agent (SAA) that is not secreted into the supernatant but is weakly associated with the cell surface and is not produced by wild-type cells (SAAs can be simple amphipathic compounds or polymers and include surfactants,which show strong surface activity and significantly reduce ST [60]). We do not believe that this SAA is viscosin, a cyclic lipopeptide surfactant known to be produced by

SBW25 which when secreted into the supernatant reduces ST down to ~33 mN m^{-1} within 24 hr [17,61] (the equal ST of cell-free culture supernatants also demonstrates that wild-type and WS cultures produce the same levels of viscosin). Instead, we suggest that this is likely to be another SAA with a stronger activity which reduces the over-all ST of WS cultures to ~31.0 mN m^{-1} (the ST of a mixture of two SAAs which do not chemically interact is the ST of the SAA with the strongest activity, i.e. the lowest ST, assuming both are present at concentrations above their critical micelle concentrations) and that this SAA allows WS cells to associate with the A-L interface far more successfully than wild-type cells.

Viscosity affects the localisation of cells at the A-L interface

In order to establish an experimental system to investigate the impact of physical disturbance on cell localisation in the high–O_2 region and colonization of the A-L interface, we established modified microcosms in which liquid viscosity had been increased. In these, both random cell diffusion and fluid flow will be reduced as they are affected by liquid viscosity [53,56,62]. We first tested the effect of adding agar, CMC, Ficol and PEG at various concentrations on wild-type cell distributions (see **Supplementary Information S4** and **Table S1** for further details). We chose agar, which increases viscosity by forming intermolecular networks (gels) [63], and PEG, which increases viscosity by intermolecular friction [64], for further experimentation and determined the viscosities of our modified microcosms by rheometry (**Table 1**). Our viscosity measurements are in agreement with other reports for agar and PEG, e.g. [65,66], and it is important to note that even at the highest concentrations of agar (0.1% w/v) and PEG (5% w/v) we chose, the modified KB medium still flowed like water and no gels or viscous solutions were formed. As some pseudomonads have been reported to utilise PEG as the sole carbon source [67-69], we tested this on wild-type SBW25 but saw no significant growth on PEG compared to the control (Dunnett's, α = 0.05). However, we noted a minor toxic effect of PEG resulting in a 0.77-fold reduction in relative growth at higher concentrations (Dunn method, $P = 0.02$), whereas agar had no significant effect (Dunn method, $P = 1.0$) (**Table 1**).

By investigating cell distributions as before, we were able to confirm quantitatively that 0.05 – 0.1 % (w/v) agar and 2.5 – 5 % (w/v) PEG significantly changed wild-type and WS cell distributions compared to standard microcosms after 24 h, with proportionally more cells localised at the top of the liquid column in the modified microcosms (TK-HSD, $\alpha = 0.05$) (**Figure 4**) (we specifically note that at the concentrations of agar and PEG used here there was no visually discernible change in liquid viscosity compared to standard microcosms). In these assays a plateauing effect on wild-type cell distribution was seen when viscosity was between 3 – 7 mPa s^{-1}, suggesting that the cells are responding to viscosity similarly, regardless of whether it is caused by inter-molecular gel formation (agar) or inter-molecular friction of monomers (PEG). WS cell distributions were ~4x higher than for the corresponding wild-type cell distributions which may reflect the increased populations Wrinkly Spreaders can achieve by biofilm–formation at the A-L interface (high PEG concentrations may also have a negative impact on WS cell distribtions though this was not significant in these assays, TK-HSD, $\alpha = 0.05$).

Increased liquid viscosity reduces the competitive advantage of biofilm–formation

We predict that Wrinkly Spreader competitive fitness should be significantly reduced as liquid viscosity is increased, to the point where wild-type cells can localise at the A-L interface in static microcosms, as under these conditions, the WS loses the advantage that biofilm–formation provides over non-biofilm–forming competitors. A significant decrease in fitness from 1.45 ± 0.06 was observed in both agar and PEG microcosms (TK-HSD, $\alpha = 0.05$) (**Figure 5a**), with fitness plateauing around one in high agar microcosms and dropping to 0.70 ± 0.04 for high PEG microcosms where the WS was at a distinct disadvantage. In contrast, in shaken microcosms where the WS cannot form a biofilm, no significant difference in fitness was found between standard and agar microcosms, although fitness in high PEG microcosms was significantly reduced (WS fitness in standard microcosms, 0.81 ± 0.01; high agar, 0.78 ± 0.02; high PEG, 0.62 ± 0.01; Dunnett's, α = 0.05), perhaps reflecting the toxic effect of high levels of PEG. The effect of increasing viscosity on WS fitness is also mirrored in diversifying populations of wild-type SBW25, where the proportion of WS cells found after 3-days also decreases significantly (TK-HSD, α = 0.05) (**Figure 5b**).

As we have previously found that Wrinkly Spreaders evolved from wild-type cells in standard microcosms or drip-feed glass-bead columns differed in terms of WS phenotype [70] (wrinklеality [12,71]), we also compared the biofilms produced in standard microcosms by a set of independent WS isolates, recovered from standard and modified microcosms, using the combined biofilm assay [37]. We found significant differences in relative strength, attachment levels and total growth between WS isolates (TK-HSD, α = 0.05) (**Figure 6**). Further analysis using a GLM approach found significant isolate[origin] and origin effects for each of these characteristics (ANOVA, $P \leq$ 0.02) and PCA could differentiate isolates from standard, high agar and high PEG microcosms (see **Supplementary Information Figure S4** for further details). This suggests that these microcosms were providing slightly different environments in which Wrinkly Spreaders are selected with subtly varying phenotypes.

DISCUSSION

Considerable growth advantages are available in the high-O_2 region of static microcosms created by the ecosystem engineering of the early wild-type SBW25 colonists [10]. This region which includes the A-L interface and extends down into the liquid column for ~1mm [10] represents an ecological opportunity for adaptive lineages such as the Wrinkly Spreaders who can occupy the 'Goldilocks zone' of optimal growth [11-12] (see [72] for the first description of bacteria occupying a region of optimal O_2 concentration) through the development of a robust biofilm at the A-L interface. This biofilm strategy is an example of resource allocation trade-off [6,73,74] as energy not required for aerotaxis is diverted away from direct growth to produce the EPS biofilm matrix that will retain cells in the high-O_2 region without constant swimming. However, as the biofilm matures greater benefits are realised as resident cells no longer have to expend energy in aerotaxis or further biofilm construction. The success of this strategy is confirmed by the competitive fitness advantage that the Wrinkly Spreaders have over non-biofilm–forming competitors [12] which will continue until growth is limited by depleted resources or when the biofilm sinks due to physical disturbance [12]. Additional confirmation of the success of the biofilm strategy is seen in the competitive fitness advantage of other A-L interface biofilms produced by SBW25 [17,19,21,22], *B. subtilis* NCIB3610 and *P. aeruginosa* PA14 [75], and more generally by the frequency of A-L interface biofilm–formation found amongst pseudomonads and other bacteria [36-40]). Nonetheless, we have been interested in understanding why biofilm–formation should be so successful at a physical level, when aerotaxis should be sufficient to gain access to the high-O_2 region and remain in place by countering the effects of physical displacement.

Our investigations have confirmed that wild-type SBW25 and the archetypal Wrinkly Spreader are aerotaxic as expected, although we note that this behaviour has been reported for very few pseudomonad strains (e.g. [76-80]) which are generally regarded as aerobic and motile [81] and aerotaxis homologues are annotated in many genomes [82]. We have also demonstrated that wild-type and WS cells are capable of accessing the high–O_2 region at the top of the liquid column of static microcosms, and the failure of *fleQ*$^-$ cells to do this confirms the importance of swimming in colonising the Goldilocks zone (motility is also important for the colonization of the A-L interface by NCIB3610 and PA14 [75]). SBW25 cells have one of the fastest swimming velocities yet reported for pseudomonads [33] and we calculate that short periods of swimming will easily overcome the effects of random cell diffusion when they are in the high–O_2 region. The presence of bioconvection currents [57] might appear to prevent the localisation of wild-type and WS cells and subsequent biofilm–formation, as cycles of aerotaxis and rest, initiates convection through instabilities and plume-formation which may transport cells far from the high–O_2 region or lead to their sedimentation. Simulations show that currents appear only above a critical culture density has been reached [62] at which point we suggest that sufficient biofilm development has occurred to withstand any further significant displacement of cells or structure (similarly these do not disrupt the formation of A-L interface biofilms by NCIB3610 and PA14 [75]; we also note that evaporation and salt accumulation at the A-L interface is sufficient to generate convection patterns in bacterial cultures [83]).

Our observations suggest that an aerotaxis-based strategy should be a plausible alternative to biofilm–formation as a means of colonising the A-L interface. However, the experimentally observed competitive fitness advantage of the Wrinkly Spreader (e.g. [14,21,50]) suggests that aerotaxis is not the optimal evolutionary solution and implies instead that biofilm–formation offers selective advantage, possibly by requiring a lower over-all energy expenditure by the growing population. Even when the cellulose biosynthesis genes are deleted, alternative A-L biofilm–forming SBW25 mutants have been isolated with competitive fitness advantages over non-biofilm–forming competitors [19,21,22]. We proposed that if biofilm–formation is the superior strategy because the main impediment to localisation in the high–O_2 region is the impact of physical displacement, WS competitive fitness relative to a non-biofilm–forming competitor should decrease as liquid viscosity was increased as random cell diffusion and fluid flow are limited by viscosity [53,56,62]. A significant decrease in WS competitive fitness and evolution was found as expected using modified microcosms in which viscosity was up to 5.7-fold higher than in standard microcosms, but far lower than what would be required to produce a visually-obvious gel or viscous solution. We also note that agar and PEG produced additional subtle effects on WS evolution, as recovered isolates exhibited distinct biofilm characteristics, suggesting that some level of local adaptation might be occurring, especially in the PEG microcosms, to reduce the impact of toxic intermediates or bottlenecks in PEG metabolism [84].

The dry-looking top surface of WS biofilms [23] has long suggested to the authors that WS cells were capable of penetrating the A-L interface (rather like bacterial meta-neustons colonising the surface microlayers of marine and freshwater habitats [41,42]), with subsequent generations pushed up above the liquid layer, and older generations gradually pushed lower down into the liquid column (resulting in an ancestor's inhibition effect [12,85]). Penetrating and crossing, or otherwise associating with the A-L interface requires mechanical energy [13], resulting in altered liquid surface tension (ST) and viscoelasticity [41,59]. This depends on bacterial surface charge and hydrophobic interactions that are also modified by cell surface features including lipopolysaccharide (LPS), other polymers and appendages, and changes to the A-L interface can in turn affect swimming behaviour through drag effects [86]. In some instances, the growth of bacteria in shaken cultures leads to an increase in ST due to the accumulation of polymers, proteinaceous material and cell debris but this can be overcome by the expression of strong surface-active agents (SAA) such as surfactants [13] which significantly reduce ST to a minimum of 23 mN m^{-1} [52,86,87] (the ST of bacterial cells can also be inferred and is affected by growth conditions and physiological state [88]).

Our comparison of the ST of wild-type and WS cultures, cell-free supernatants and washed cells suggest that Wrinkly Spreaders are expressing a SAA weakly associated with the cell surface, which allows better penetration of the A-L interface than for wild-type cells. Further work will be required to identify the SAA which could be cellulose [14,23] or PNAG [21] attachment factor, both of which are over-expressed by Wrinkly Spreaders but expressed at low levels by wild-type cells, or possible a completely new component not yet associated with the WS phenotype. Changes in the expression of cell surface features such as cellulose and LPS are known to affect WS relative cell hydrophobicity and recruitment levels to the A-L interface [24]. Various types of cellulose fibres and derivatives are known to alter ST, e.g. [89-92], and in earlier work we demonstrated that that cellulose-expression by wild-type SBW25 could explain the reduction of ST from ~27 to 25 mN m^{-1} [17], but we are not aware of any publications demonstrating the same for PNAG. However, an alternative explanation is that the Wrinkly Spreader expresses another SAA which is more tightly repressed in wild-type cells. We have previously suggested that a highly-hydrophobic amyloid fibre potentially expressed by *fabA–F* homologues (PFLU2701– 2696) is a likely candidate involved in attachment [12,93,94] which might also allow better penetration of the A-L interface. Amyloid fibres allow the gelation of polysaccharides and result in modified matrices with different viscoelastic properties [95] and these fibres need to penetrate the A-L interface in order to form a robust biofilm [96]. Such fibres might explain the difference seen between the dry-looking and robust WS biofilm and the wet-looking VM biofilm produced by wild-type SBW25 [17] which readily sinks when disturbed but nonetheless is still associated with the A-L interface [59].

We have a long-term interest in understanding the underlying molecular biology and evolutionary ecology of the Wrinkly Spreader [12]. Our investigation of how wild-type and WS cells access and remain in the high-O_2 region highlights the advantage biofilm-formation has over aerotaxis in overcoming displacement from this Goldilocks zone of optimal growth [11,12], and the difficulty in penetrating the A-L interface, which allows the development of substantially larger and more robust biofilms. Although biofilm-formation has been identified as the key innovation of the Wrinkly Spreader [14], we now raise the question of whether the key is really the ability to cross the A-L interface and avoid the energetic costs involved in maintaining position in the high-O_2 region, rather than the subsequent population increase across the A-L interface in the developing biofilm.

SUPPORTING INFORMATION AND DATA

Supporting information is available as a Supplementary Information file. Data are available from Mendeley Data (http://dx.doi.org/10.17632/rwh8vchkxg.1).

AUTHOR STATEMENTS

ORCID Author identifiers: Robyn Jerdan, 0000-0002-7045-8362; Anna Kuśmierska, 0000-0003-1214-4549; Marija Petric, 0000-0001-8588-9870; Andrew Spiers, 0000-0003-0463-8629. Roles undertaken: R. Jerdan: Design, experimentation, analysis and manuscript development; A. Kuśmierska: Experimentation; M. Petric: Experimentation; A. Spiers: Design, experimentation, analysis, manuscript development and supervision. All authors contributed to the final manuscript preparation.

CONFLICTS OF INTERESTS

The authors declare that there are no conflicts of interests.

FUNDING INFORMATION

This research was funded by Abertay University which is a charity registered in Scotland, No. SC016040. Anna Kuśmierska's visit to Abertay was supported by the European Region Action Scheme for the Mobility of University Students (Erasmus) Programme, and Marija Petric by the International Association for the Exchange of Students for Technical Experience (IAESTE) Programme and the British Council.

ACKNOWLEDGEMENTS

We would like to thank Neil Cunningham of the Centre for Industrial Rheology for his help in determining media viscosities, Nia White for her comments on the final draft manuscript, and the two anonymous referees for their critical reviews. Andrew Spiers is also member of the Scottish Alliance for Geoscience Environment and Society (SAGES).

REFERENCES

[1] **Schulter D.** The ecology of adaptive radiation. Oxford: Oxford University Press; 2000.

[2] **Losos JB, Mahler DL.** Adaptive Radiation: The Interaction of Ecological Opportunity, Adaptation, and Speciation. In: Bell MA, Futuyma DJ, Eanes WF, and Levinton JS (editors). *Evolution Since Darwin: The First 150 Years*. Sunderland: Sinauer Assoc.; 2010. pp. 381–420.

[3] **Buckling A, Maclean RC, Brockhurst MA, Colegrave N.** The Beagle in a bottle. *Nature* 2009;457:824–829.

[4] **Kawecki TJ, Lenski RE, Ebert D, Hollis B, Olivieri I, Whitlock MC.** Experimental evolution. *Trends Evolution* 2012;27:547–560.

[5] **Dykhuizen D.** Thoughts toward a theory of Natural Selection: The importance of microbial experimental evolution. *Cold Spring Harb Perspect Biol* 2016;8:a018044.

[6] **Bachmann H, Molenaar D, dos Santos FP, Teusink B.** Experimental evolution and the adjustment of metabolic strategies in lactic acid bacteria. *FEMS Microbiol Rev* 2017;41(Supp_1):S201–S219.

[7] **Bailey MJ, Thompson IP.** Detection systems for phyllosphere Pseudomonads. In: Wellington EMR and van Elsas JD (editors). *Genetic Interactions Between Microorganisms in the Natural Environment*. Oxford: Pergamon Press; 1992. pp. 127–141.

[8] **Rainey PB, Bailey MJ.** Physical and genetic map of the *Pseudomonas fluorescens* SBW25 chromosome. *Mol Microbiol* 1996;19:521–33.

[9] **Rainey PB, Travisano T.** Adaptive radiation in a heterogeneous environment. *Nature* 1998;394:69–72.

[10] **Koza A, Moshynets O, Otten W, Spiers AJ.** Environmental modification and niche construction: developing O_2 gradients drive the evolution of the Wrinkly Spreader. *ISME J* 2011;5:665–73.

[11] **Kuśmierska A, Spiers AJ.** New insights into the effects of several environmental parameters on the relative fitness of a numerically dominant class of evolved niche specialist. *Int J Evolutionary Biol* 2016;4846565.

[12] **Koza A, Kuśmierska A, McLaughlin K, Moshynets O, Spiers AJ.** Adaptive radiation of *Pseudomonas fluorescens* SBW25 in experimental microcosms provides an understanding of the evolutionary ecology and molecular biology of A-L interface biofilm formation. *FEMS Microbiology Lett* 2017;364:fnx109.

[13] **Berg JC.** Fluid interfaces and capillarity. In: Berg JC. *An Introduction to Interfaces and Colloids.* Singapore: World Scientific Publishing Co.; 2009. pp. 23–106.

[14] **Spiers AJ, Kahn SG, Bohannon J, Travisano M, Rainey PB.** Adaptive divergence in experimental populations of *Pseudomonas fluorescens*. I. Genetic and phenotypic bases of Wrinkly Spreader fitness. *Genetics* 2002;161:33-46.

[15] **Moshynets OV, Spiers AJ.** Viewing biofilms within the larger context of bacterial aggregations. In: Dhanasekaran D and Thajuddin N (editors). *Microbial biofilms.* Rijeka: InTech Publishers; 2016. pp. 3–22.

[16] **Spiers AJ.** A mechanistic explanation linking adaptive mutation, niche change, and fitness advantage for the Wrinkly Spreader. *Int J Evolionary Biol* 2014;675432.

[17] **Koza A, Hallett PD, Moon CD, Spiers AJ.** Characterisation of a novel air–liquid interface biofilm of *Pseudomonas fluorescens* SBW25. *Microbiol* 2009;155:1397–1406.

[18] **Bantinaki B, Kassen R, Knight CG, Robinson Z, Spiers AJ, Rainey PB.** Adaptive divergence in experimental populations of *Pseudomonas fluorescens*. III. Mutational origins of Wrinkly Spreader diversity. *Genetics* 2007;176:441–453.

[19] **McDonald MJ, Gehrig SM, Meintjes PL, Zhang X-X, Rainey PB.** Adaptive divergence in experimental populations of *Pseudomonas fluorescens*. IV. Genetic constraints guide evolutionary trajectories in a parallel adaptive radiation. *Genetics* 2009;183:1041–1053.

[20] **McDonald MJ, Cooper TF, Beaumont HJE, Rainey PB.** The distribution of fitness effects of new beneficial mutations in *Pseudomonas fluorescens. Biol Lett* 2011;7:98100.

[21] **Lind PA, Farr AD, Rainey PB.** Experimental evolution reveals hidden diversity in evolutionary pathways. *eLife* 2015;4:e07074.

[22] **Lind PA, Farr AD, Rainey PB.** Evolutionary convergence in experimental *Pseudomonas* populations. *ISME J* 2017;11:589–600.

[23] **Spiers AJ, Bohannon J, Gehrig S, Rainey PB.** Biofilm formation at the air–liquid interface by the *Pseudomonas fluorescens* SBW25 wrinkly spreader requires an acetylated form of cellulose. *Molec Microbiol* 2003;50:15–27.

[24] **Spiers AJ, Rainey PB.** The *Pseudomonas fluorescens* SBW25 wrinkly spreader biofilm requires attachment factor, cellulose fibre and LPS interactions to maintain strength and integrity. *Microbiology* 2005;151:2829–39.

[25] **Arber W.** Genetic variation: molecular mechanisms and impact on microbial evolution. *FEMS Microbiol Reviews* 2000;24:1–7.

[26] **Andersson DI, Jerlström-Hultqvist J, Näsvall J.** Evolution of new functions de novo and from preexisting genes. *Cold Spring Harb Perspect Biol* 2015;7:a017996.

[27] **Johnson AD.** The rewiring of transcription circuits in evolution. *Current Opin Genetics Devel* 2017;47:121–127.

[28] **Taylor BL, Zhulin IB, Johnson MS.** Aerotaxis and other energy-sensing behaviour in bacteria. *Annu Rev Microbiol* 1999;53:103–28.

[29] **Bailey MJ, Lilley AK, Thompson IP, Rainey PB, Ellis RJ.** Site directed chromosomal marking of a fluorescent Pseudomonad isolated from the phytosphere of sugar beet, stability and potential for marker gene transfer. *Mol Ecol* 1995;4:755–763.

[30] **Turnbull GA, Morgan JAW, Whipps JM, Saunders JR.** The role of bacterial motility in the survival and spread of *Pseudomonas fluorescens* in soil and in the attachment and colonisation of wheat roots. *FEMS Microbiol Ecol* 2001;36:21–31.

[31] **De Weert S, Vermeiren H, Mulders IHM, Kuiper I, Hendrickx N, Bloemberg GV, Vanderleyden J, De Mot R, Lugtenberg BJJ.** Flagella-driven chemotaxis towards exudate components is an important trait for Tomato root colonization by *Pseudomonas fluorescens*. *MPMI* 2002;15:1173–1180.

[32] **Jones J, Studholme DJ, Knight CG, Preston GM.** Integrated bioinformatic and phenotypic analysis of RpoN-dependent traits in the plant growth-promoting bacterium *Pseudomonas fluorescens* SBW25. *Environ Microbiol* 2007;9:3046–3064.

[33] **Ping L, Birkenbeil J, Monajembashi S.** Swimming behaviour of the monotrichous bacterium *Pseudomonas fluorescens* SBW25. *FEMS Microbiol Ecol* 2013; 86:36–44.

[34] **Alsohim AS, Taylor TB, Barrett GA, Gallie J, Zhang X-X, Altamirano-Junqueira AE, Johnson, LJ, Rainey PB, Jackson RW.** The biosurfactant viscosin produced by *Pseudomonas fluorescens* SBW25 aids spreading motility and plant growth promotion. *Environ Microbiol* 2014;16:2267–2281.

[35] **Silby MW, Cerdeño-Tárraga AM, Vernikos G, Giddens SR, Jackson R, Preston G, Zhang X-X, Godfrey S, Spiers AJ, Harris S, Challis GL, Morningstar A, Harris D, Seeger K, Murphy L, Rutter S, Squares R, Quail MA, Saunders E, Anderson I, Mavromat K, Brettin TS, Bentley S, Thomas CM, Parkhill J, Levy SB, Rainey PB, Thomson NR.** Genomic and genetic analyses of diversity and plant interactions of *Pseudomonas fluorescens*. *Genome Biology* 2009;10:R51.

[36] **Ude S, Arnold DL, Moon CD, Timms-Wilson T, Spiers AJ.** Biofilm formation and cellulose expression among diverse environmental *Pseudomonas* isolates. *Environ Microbiol* 2006; 8:1997–2011.

[37] **Robertson M, Hapca SM, Moshynets O, Spiers AJ.** Air-liquid interface biofilm formation by psychrotrophic pseudomonads recovered from spoilt meat. *Antonie van Leeuwenhoek* 2013;103:251–259.

[38] **Ueda A, Saneoka H.** Characterization of the ability to form biofilms by plant-associated *Pseudomonas* species. *Curr Microbiol* 2015;70:506–513.

[39] **Armitano J, Méjean V, Jourlin-Castelli C.** Gram-negative bacteria can also form pellicles. *Environ Microbiol Reports* 2014;6:534–544.

[40] **Vlamakis H, Chai Y, Beauregard P, Losick R, Kolter R.** Sticking together: building a biofilm the *Bacillus subtilis* way. *Nat Rev Microbiol* 2013;11:157–168.

[41] **Kjelleberg S.** Mechanisms of bacterial adhesion at gas-liquid interfaces. In: Fletcher M and Savage DC (editors). *Bacterial adhesion: Mechanisms and Physiological Significance.* New York: Plenum Press; 1985. pp. 163–194.

[42] **Marshall HG, Burchardt L.** Neuston: its definition with a historical review regarding its concept and community structure. *Archiv fur Hydrobiologie* 2005;164:429–448.

[43] **Wotton RS, Preston TM.** Surface films: areas of water bodies that are often overlooked. *Bioscience* 2005;55:137–145.

[44] **Cunliffe M, Upstill-Goddard RC, Murrell JC.** Microbiology of aquatic surface microlayers. *FEMS Microbiol Rev* 2011;35:233–246.

[45] **Spiers AJ, Arnold DL, Moon CD, Timms-Wilson.** A survey of A-L biofilm formation and cellulose expression amongst soil and plant-associated Pseudomonas isolates. In: *Microbial Ecology of Aerial Plant Surfaces.* Bailey MJ, Lilley AK, Timms-Wilson TM (Eds). Wallingford: CABI; 2006. pp. 121–132.

[46] **Holden PA.** How do the microhabitats framed by soil structure impact soil bacteria and the processes they regulate? In: Ritz K, Young I (editors). *The architecture and biology of soils.* Wallingford: CABI; 2011. pp. 118–148.

[47] **King EO, Ward MK, Raney DC.** Two simple media for the demonstration of pyocyanin and fluorescin. *J Labor Clin Med* 1954;44:301–307.

[48] **Sambrook J, Fritsch EF, Maniatis T.** *Molecular Cloning. A Laboratory Manual.* 2nd Edition. Cold Spring Harbor: Cold Spring Harbor Laboratory Press; 1989.

[49] **Gates FL, Olitsky PK.** Factors influencing anaerobiosis, with special reference to the use of fresh tissue. *J Exp Med* 1921;33:51–68.

[50] **Green JH, Koza A, Moshynets O, Pajor P, Ritchie MR, Spiers AJ.** Evolution in a Test-tube: Rise of the Wrinkly Spreaders. *J Biol Educ* 2011;45:54–59.

[51] **Lenski RE, Rose MR, Simpson SC, Tadler SC.** Long-term experimental evolution in *Escherichia coli.* I. Adaptation and divergence during 2,000 generations. *Amer Naturalist* 1991;138:1315–1341.

[52] **Fechtner J, Koza A, Dello Sterpaio P, Hapca SM, Spiers AJ.** Surfactants expressed by soil pseudomonads alter local soil-water distribution, suggesting a hydrological role for these compounds. *FEMS Microbiol Ecol* 2011;78:50–58.

[53] **Berg HC.** Movement of self-propelled objects. In: Berg HC (editor). *Random walks in biology*. Expanded edition. Princetown: Princetown University Press; 1993. pp. 75–93.

[54] **Jørgensen BB.** Life in the diffusive boundary layer. In: Boudreau BP and Jørgensen BB (editors). *The benthic boundary layer. Transport processes and biogeochemistry.* Oxford: Oxford University Press; 2001. pp. 348–373.

[55] **Giddens SR, Jackson RW, Moon CD, Jacobs MA, Zhang X-X, Gehrig SM, Rainey PB.** Mutational activation of niche-specific genes provides insight into regulatory networks and bacterial function in a complex environment. *PNAS (USA)* 2007;104:18247–18252.

[56] **Pedley TJ, Kessler JO.** Hydrodynamic phenomena in suspensions of swimming microorganisms. *Annu Rev Fluid Mech* 1992;24:313–358.

[57] **Ardré M, Dufour D, Rainey PB.** Causes and biophysical consequences of cellulose production by *Pseudomonas fluorescens* SBW25 at the air-liquid interface. In press, May 13, J Bacteriol 2019.

[58] **Kjelleberg S, Stenström TA.** Lipid surface films: interaction of bacteria with free fatty acids and phospholipids at the air/water interface. *J Gen Microbiology* 1980;116:417–423.

[59] **Rühs PA, Böni L, Fuller GG, Inglis RF, Fisher P.** In-situ quantification of the interfacial rheological response of bacterial biofilms to environmental stimuli. *PLoS ONE* 2013;8:e78524.

[60] **Holmberg K, Jönsson B, Kronsberg B, Lindman B.** Surfactants and polymers in aqueous solution. 2nd Ed. Chichester: John Wiley and Sons, Ltd.; 2002.

[61] **de Bruijn I, de Kock MJD, Yang M, de Waard P, van Beek TA, Raaijmakers JM.** Genome-based discovery, structure prediction and functional analysis of cyclic lipopeptide antibiotics in *Pseudomonas* species. *Mol Microbiol* 2007;63:417–428.

[62] **Deleuze Y, Chiang C-Y, Thiriet M, Sheu TWH.** Numerical study of plume patterns in a chemotaxis-diffusion-convection coupling system. *Computers Fluids* 2016;126:58–70.

[63] **Armisén R, Galatas F.** Agar. In: Phillips GO, Williams PA (editors). *Handbook of hydrocolloids.* Cambridge: Woodhead Publishing Ltd; 2009 (2nd Ed). pp. 82–203.

[64] **Zhao Z, Ji X, Dimova R, Lipowsky R, Liu Y.** Viscoelasticity of poly(ethylene glycol) solutions on supported lipid bilayers via quartz crystal microbalance with dissipation. *Macromolecules* 2015;48:1824–1831.

[65] **Kirincica S, Klofutar C.** Viscosity of aqueous solutions of poly(ethylene glycol)s at 298.15 K. *Fluid Phase Equilibria* 1999:155:311–325.

[66] **Asyakin LK, Dyshlyuk LS.** Study of viscosity of aqueous solutions of natural polysaccharides. *Science Evolution* 2016;1:11–19.

[67] **Haines JR, Alexander M.** Microbial degradation of polyethylene glycols. *Appl Microbiol* 1975;29:621–625.

[68] **Obradors N, Aguilar J.** Efficient biodegradation of high-molecular-weight polyethylene glycols by pure cultures of *Pseudomonas stutzeri*. *AEM* 1991;57:2383–2388.

[69] **Hu X, Fukutani A, Liu X, Kimbara K, Kawai F.** Isolation of bacteria able to grow on both polyethylene glycol (PEG) and polypropylene glycol (PPG) and their PEG/PPG dehydrogenases. *Appl Microbiol Biotechnol* 2007;73:1407–1413.

[70] **Udall YC, Deeni Y, Hapca SM, Raikes D, Spiers AJ.** The evolution of biofilm-forming Wrinkly Spreaders in static microcosms and drip-fed columns selects for subtle differences in wrinkleality and fitness. *FEMS Microbiol Ecol* 2015;91:fiv057.

[71] **Spiers AJ.** Bacterial evolution in simple microcosms. In: Harris CH (editor). *Microcosms: Ecology, Biological Implications and Environmental Impact.* Hauppauge: Nova Publishers; 2013.

[72] **Jennings HS, Crosby JH.** Studies on reactions to stimuli in unicellular organisms. VII. The manner in which bacteria react to stimuli, especially to chemical stimuli. *Amer J Physiology* 1901;6:31–37.

[73] **Acerenza L.** Constraints, Trade-offs and the currency of fitness. *J Mol Evol* 2016;82:117–127.

[74] **Ferenci T.** Trade-off mechanisms shaping the diversity of bacteria. *Trends Microbiol* 2016;24:209–223.

[75] **Hölscher T, Bartels B, Lin Y-C, Gallegos-Monterrosa R, Price-Whelan A, Kolter R, Dietrich LEP, Kovács ÁT.** Motility, chemotaxis and aerotaxis contribute to competitiveness during bacterial pellicle biofilm development. *J Mol Biol* (2015;427:3695–3708.

[76] **Kelman A, Hruschka J.** The role of mobility and aerotaxis in the selective increase of avirulent bacteria in still broth cultures of *Pseudomonas solanacearum*. *J Gen Microbiol* 1973:76:177–188.

[77] **Nichols NN, Harwood CS.** An aerotaxis transducer gene from *Pseudomonas putida*. *FEMS Microbiol Lett* 2000;182:177–183.

[78] **Shitashiro M, Kato J, Fukumura T, Kuroda A, Ikeda T, Takiguchi N, Ohtake H.** Evaluation of bacterial aerotaxis for its potential use in detecting the toxicity of chemicals to microorganisms. *J Biotechnol* 2003;101:11–18.

[79] **Sarand I, Österberg S, Holmqvist S, Holmfeldt P, Skärfstad E, Parales RE, Shingler V.** Metabolism-dependent taxis towards (methyl)phenols is coupled through the most abundant of three polar localized Aer-like proteins of *Pseudomonas putida*. *Environ Microbiol* 2008;10:1320–1334.

[80] **Muriel C, Jalvo B, Redondo-Nieto M, Rivilla R, Martín M.** Chemotactic motility of *Pseudomonas fluorescens* F113 under aerobic and denitrification conditions. PLoS ONE 2015;10: e0132242.

[81] **Brenner DJ, Krieg NR, Staely JT, Garrity GM**. *Bergy's manual of systematic bacteriology.* 2nd ed, vol. 2, part B. New York: Spinger-Verlag; 2005. pp. 323–378.

[82] **Sampedro I, Parales RE, Krell T, Hill JE.** *Pseudomonas* chemotaxis. FEMS Microbiol Rev 2015;39:17–46.

[83] **Dunstan J, Lee KJ, Hwang Y, Park SF, Goldstein RE.** Evaporation-driven convective flows in suspensions of nonmotile bacteria. *Physical Rev Fluids* 2018;3;123102.

[84] **Franden MA, Jayakody LN, Li WJ, Wagner NJ, Cleveland NS, Michener WE, Hauer B, Blank LM, Wierckx N, Klebensberger J, Beckham GT.** Engineering *Pseudomonas putida* KT2440 for efficient ethylene glycol utilization. *Metabolic Engineering* 2018;48:198–207.

[85] **Xavier JB, Foster KR.** Cooperation and conflict in microbial biofilms. *PNAS USA* 2007;104:876–81.

[86] **Morse M, Huang A, Li G, Maxey MR, Tang JX.** Molecular adsorption steers bacterial swimming at the air/water interface. *Biophysical J* 2013;105:21–28.

[87] **Fechhner J, Cameron S, Deeni YY, Hapca SM, Kabir K, Mohammed IU, Spiers AJ.** Limitations of biosurfactant strength produced by bacteria. In: Upton RC (editor). *Biosurfactants Occurrences, applications and research.* New York: NOVA Science Publishers; 2017. pp. 125–148.

[88] **Strevett KA, Chen G.** Microbial surface thermodynamics and applications. *Res Microbiology* 2003;154:329–335.

[89] **Ardizzone S, Dioguardi FS, Quagliotto P, Vercelli B, Viscardi G.** Microcrystalline cellulose suspensions: effects on the surface tension at the air–water boundary. *Colloids Surf A: Physicochem Engin Aspects* 2001:176;239–244.

[90] **Stana-Kleinschek K, Ribitsch V, Kreze T, Fras L.** Determination of the adsorption character of cellulose fibres using surface tension and surface charge. *Mat Res Innovat* 2002;6:13–18.

[91] **Nasatto PL, Pignon F, Silveira JLM, Duarte MER, Noseda MD, Rinaudo M.** Interfacial properties of methylcelluloses: the influence of molar mass. *Polymers* 2014;6:2961–2973.

[92] **Jilal I, El Barkany S, Bahari Z, El Idrissi A, Salhi A, Abou-Salama M, Ahari M, Amhamdi H.** A new equation between surface tension and solubility parameters of cellulose derivatives depending on DS: Application on cellulose acetate. *Appl Envir Eng Sci* 2018;4:171–181.

[93] **Dueholm MS, Otzen D, Nielsen PH.** Evolutionary insight into the functional amyloids of the pseudomonads. *PLoS One* 2013;8:e76630.

[94] **Taglialegna A, Lasa I, Valle J.** Amyloid structures as biofilm matrix scaffolds. *J Bacteriol* 2016;198:2579–2588.

[95] **Lembré P, Di Martino P, Vendrely C.** Amyloid peptides derived from CsgA and FapC modify the viscoelastic properties of biofilm model matrices. *Biofouling* 2014;30:415–426.

[96] **Wu C, Lim JY, Fuller GG, Cegelski L.** Disruption of *Escherichia coli* amyloid-integrated biofilm formation at the air−liquid interface by a polysorbate surfactant. *Langmuir* 2013;29:920–926.

FIGURE LEGENDS

Figure 1. **Wild-type SBW25 and Wrinkly Spreader cells are aerotaxic.** The O_2-directed flagella-mediated swimming (i.e. aerotaxis) behaviour of wild-type cells can be visualised by monitoring cell migration in soft-agar (a). After 48 hr cells have moved towards the source of O_2 (i.e. the open end of the test tube) (top arrow) following the O_2 gradient, rather than downwards to the sealed end of the test tube (tetrazolium violet has been added to help visualise live-cells; a lot of the initial inoculum remains at the mid-point and probably represents dead cells). Aerotaxis behaviour can also be quantified by determining cell distributions along an A-L interface in a microscope chamber (b). Shown here are images of the same chamber under O_2-depleted conditions and then after 30 min re-equilibration with normal O_2 levels in which more wild-type cells are located near to the A-L interface. Cell distributions derived from microscope images can be used to quantify the aerotaxis behaviour of wild-type and WS cells compared to non-motile *fleQ*$^-$ cells which are not capable of aerotaxis *ipso facto* (c). Cell distributions were determined from paired images taken under O_2-depleted conditions and then after 30 min re-equilibration with normal O_2 levels and is shown as the O_2 / N_2 cell number ratio. A ratio significantly greater than one (grey line) suggests that cells are aerotaxic. Means (black circles) ± SE are shown (replicates are indicated by white circles). Means not linked by the same letter are significantly different (TK-HSD, α = 0.05). Wild-type and WS O_2 / N_2 cell number ratios are significantly different to one (T-test, $P > 0.05$) but the *fleQ*$^-$ ratio is not ($P = 0.33$).

Figure 2. **Wrinkly Spreader cells show higher levels of enrichment in the O_2-rich top layer of the liquid column than either wild-type or non-motile *fleQ*$^-$ cells.** Localisation at the

top of the liquid column requires aerotaxis capable of overcoming random cell diffusion, microcurrents and physical disturbance, and cell sedimentation. Wild-type SBW25 cells are enriched at the top of the liquid column (a) compared to non-aerotaxic (and non-swimming) *fleQ*$^{-}$ mutant cells, which sediment at the bottom of the liquid column (b). In comparison, WS cells show even higher levels of enrichment at the top compared (c) to wild-type cells. Cell distributions were determined from OD_{600} measurements of six 1 ml samples taken from the top down to the bottom of static microcosms 24 h after vigorous mixing to produce a uniform distribution of cells throughout the liquid column. Control measurements were taken from a separate set of mixed microcosms incubated for the same period but re-mixed before sampling. Cell distributions are shown as the cell distributions in the liquid column (sample at a particular depth / mixed control OD_{600} ratio). A ratio of one suggests cells are equally distributed throughout the liquid column. Means (black circles) ± SE are shown (replicates are indicated by white circles). Means not linked by the same letter are significantly different (TK-HSD, $\alpha = 0.05$). Trend lines (dashed curves) are descriptive only.

Figure 3 **Wrinkly Spreader cultures have lower surface tensions than wild-type SBW25.** Surface tension (ST, mM m^{-1}) measurements can be used to investigate the association with and penetration of cells into and across the A-L interface through cell surface features including attached and loosely-associated polymers. Shown here is a comparison of ST measurements from cultures, cell-free culture supernatants and vigorously-washed and re-suspended wild-type and WS cells. Means (black circles) ± SE are shown (replicates are indicated by white circles). Means not linked by the same letter are significantly different (TK-HSD, $\alpha = 0.05$). Further investigation showed a significant difference (*) between mean wild-type and WS culture ST (T-test, $P = 0.02$) but not between washed cells (T-test, $P = 0.18$) or supernatants (T-test, $P = 0.16$).

Figure 4. **Cell localisation to the high-O_2 region is sensitive to liquid viscosity.** Random cell diffusion, bioconvection currents and physical disturbance (i.e. displacement) all affect the distribution of wild-type (circles) and WS (squares) cells in the liquid column of static microcosms. However, the relative impact of these factors can be reduced by increasing liquid viscosity, which results in more cells being localised to the high-O_2 region at the top of the liquid column. Standard microcosms (white) were modified by the addition of agar (grey) or PEG (black) to increase viscosity. Cell distributions were determined from OD_{600} measurements of samples taken from the bottom of static microcosms and after vigorous mixing and is shown as the cell distributions in the liquid column (mixed / bottom OD_{600} ratio). A ratio less than one suggests that fewer cells are at that depth compared to the mixed control. Means (large symbols) ± SE are shown (replicates are indicated by small symbols). Means not linked by the same letter are significantly different (TK-HSD, $\alpha = 0.05$). Trend lines (dashed curves) are descriptive only.

Figure 5. **WS fitness is affected by viscosity.** The competitive fitness (W) of the archetypal Wrinkly Spreader compared to the non-biofilm–forming wild-type SBW25 decreases with increasing liquid viscosity (a). A competitive fitness of one (grey line) indicates that the WS and wild-type have no advantage over one another; higher values indicate a WS advantage and lower values a wild-type advantage. This reduction is also reflected in the percentage of WS cells found in diversifying wild-type populations after 3 days (b). Standard microcosms (white circles) were modified by the addition of agar (grey circles) or PEG (black circles) to increase viscosity. Means (large symbols) ± SE are

shown (replicates are indicated by small symbols). Means not linked by the same letter are significantly different (TK-HSD, $\alpha = 0.05$). Data are jigged horizontally to avoid over-laps. Trend lines (dashed curves) are descriptive only.

Figure 6. **Wrinkly Spreaders evolved in modified microcosms have different biofilm characteristics.** The combined biofilm assay was used to characterise the biofilms produced in standard microcosms by 25 independent Wrinkly Spreader isolates recovered from standard and modified microcosms containing low and high concentrations of agar and PEG. Shown are relative biofilm strengths measured using small galls balls (grams) (a), attachment levels measured by Crystal violet staining (A_{570}) (b), and total microcosm growth (OD_{600}) (c). The relative value of one (grey line) is the mean of all measurements ($n = 125$). Means (black circles) ± SE are shown (mean data from individual Wrinkly Spreader isolates are indicated by white circles). Means not linked by the same letter are significantly different (LSMeans Differences Tukey HSD, $\alpha = 0.05$).

TABLE

Table 1. Viscosity and growth characteristics of microcosms with added agar and polyethylene glycol (PEG).

Microcosm	Concentration (w/v %)	Viscosity (mPa s)	Localisation to the top	Growth (OD_{600})
Standard	-	1.26 ± 0.02 [a]	No	1.45 ± 0.05 (1.00)
Low agar	0.01	1.56 [†]	No	1.25 ± 0.05 (0.86)
Medium agar	0.05	2.74 ± 0.02 [b]	Yes	1.34 ± 0.04 (0.92)

High agar	0.1	7.13 ± 0.24 [c]	Yes	1.33 ± 0.02 (0.92)
Low PEG	1	1.44 [†]	No	1.23 ± 0.07 (0.85)
Medium PEG	2.5	1.71 ± 0.02 [a]	Yes	1.16 ± 0.06 (0.80)
High PEG	5	2.75 ± 0.14 [b]	Yes	1.11 ± 0.06 (0.77) [*]

Means ± SE are shown for measurements of viscosity and wild-type SBW25 growth. †, Viscosity for low concentrations were interpolated assuming a simple linear relationship. Visually-obvious agar gelling occurred at 0.3% (w/v) agar and PEG solutions of 20% (w/v) were very difficult to pour. Relative growth compared to standard microcosms is shown in parentheses. Viscosity means not linked by the same letter are significantly different (TK-HSD, $\alpha = 0.05$). Growth means are not significantly different (Dunn method, $P > 0.05$) except where indicated (*) ($P = 0.02$).

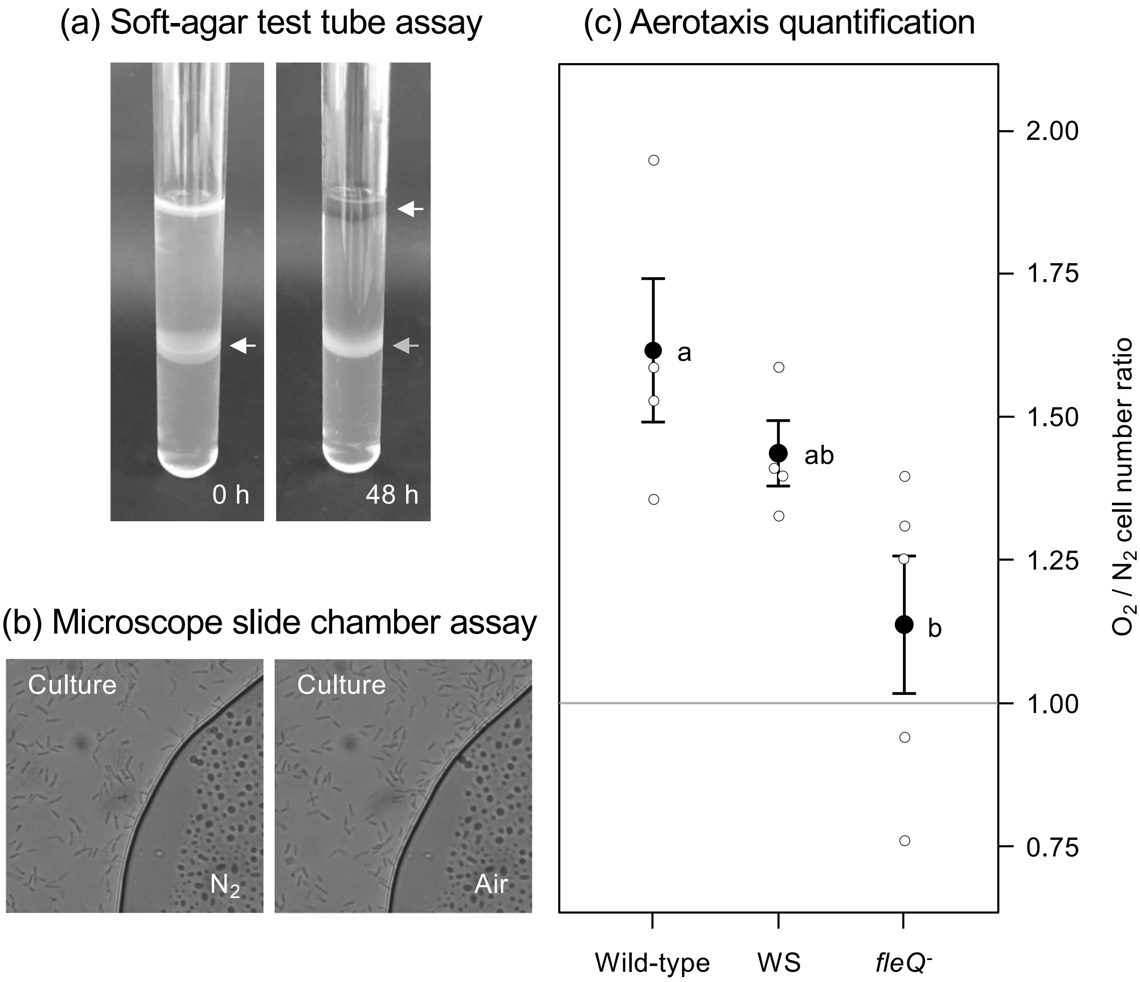
(a) Soft-agar test tube assay
0 h
48 h
(b) Microscope slide chamber assay
Culture
Culture
N_2
Air
(c) Aerotaxis quantification
2.00
1.75
1.50
1.25
1.00
0.75
O_2 / N_2 cell number ratio
a
ab
b
Wild-type
WS
fleQ-

Figure 1

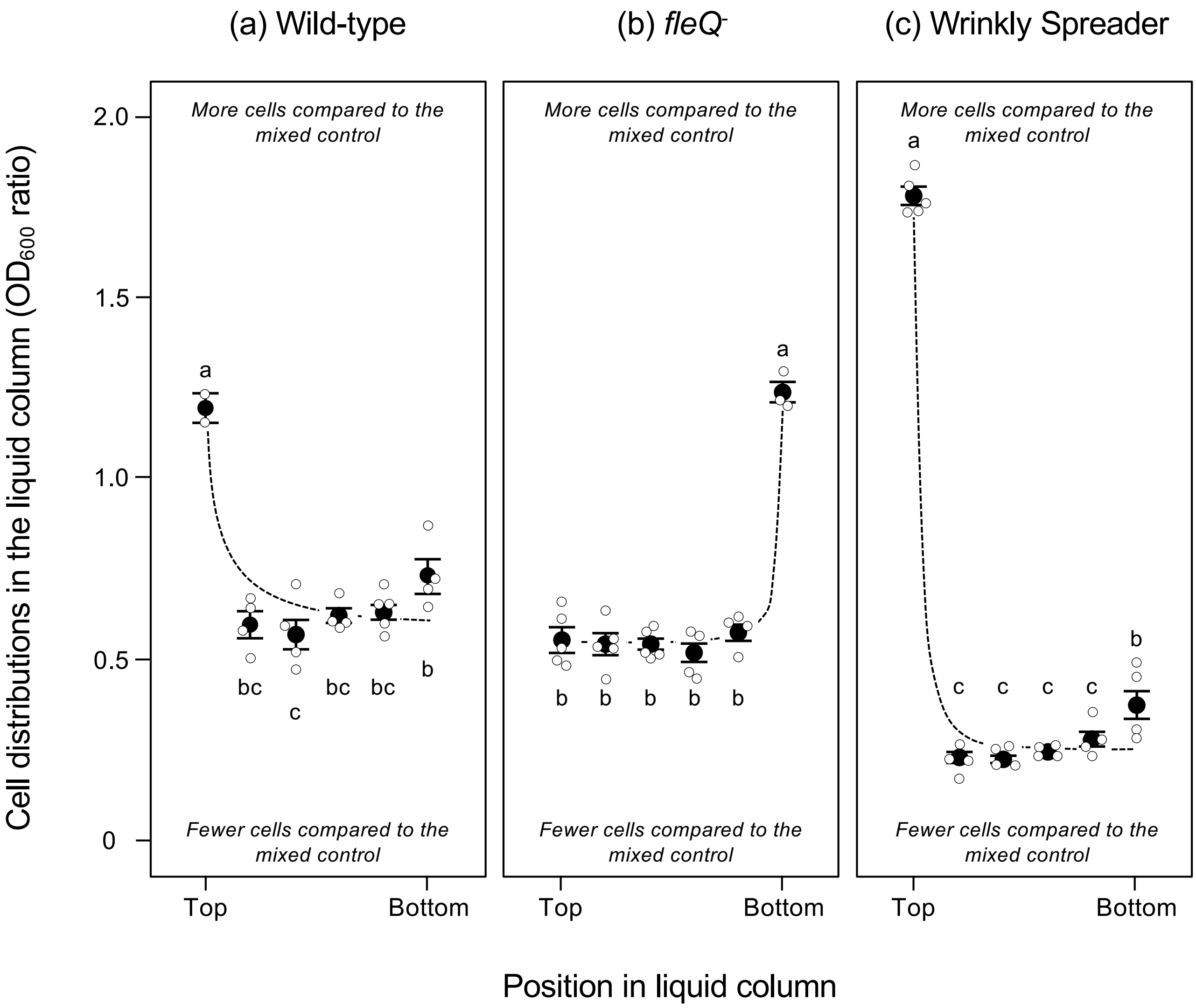
(a) Wild-type
(b) fleQ-
(c) Wrinkly Spreader
More cells compared to the mixed control
Fewer cells compared to the mixed control
Cell distributions in the liquid column (OD600 ratio)
Position in liquid column
Top
Bottom
2.0
1.5
1.0
0.5
0
a
bc
c
b

Figure 2

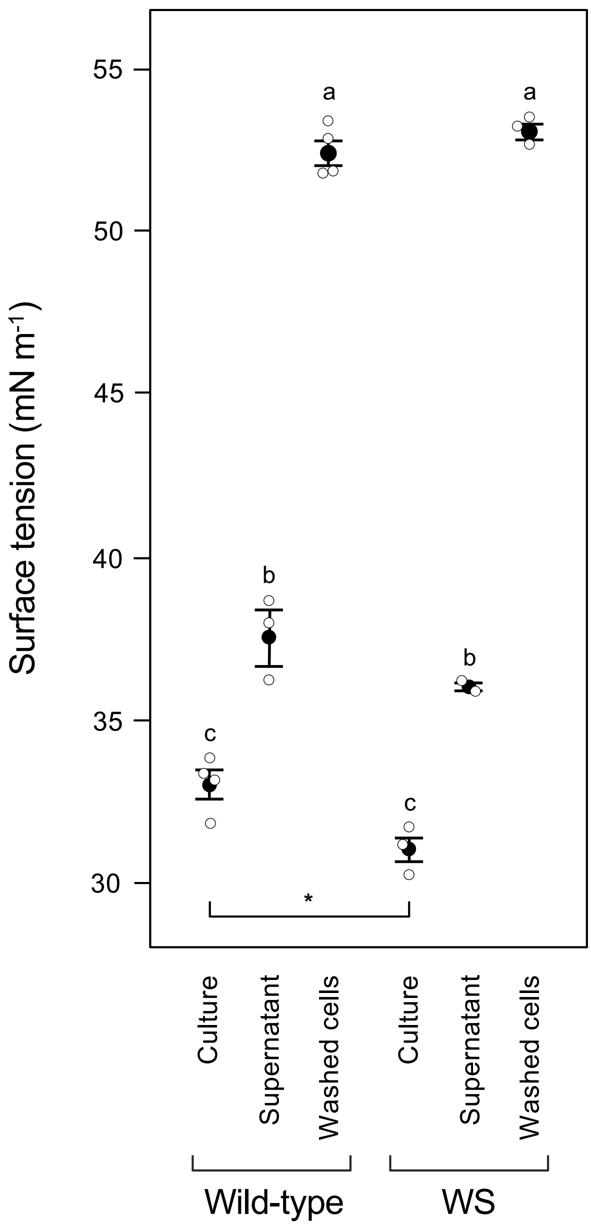

Surface tension (mN m⁻¹)
55
50
45
40
35
30
a
a
b
b
c
c
*
Culture
Supernatant
Washed cells
Culture
Supernatant
Washed cells
Wild-type
WS

Figure 3

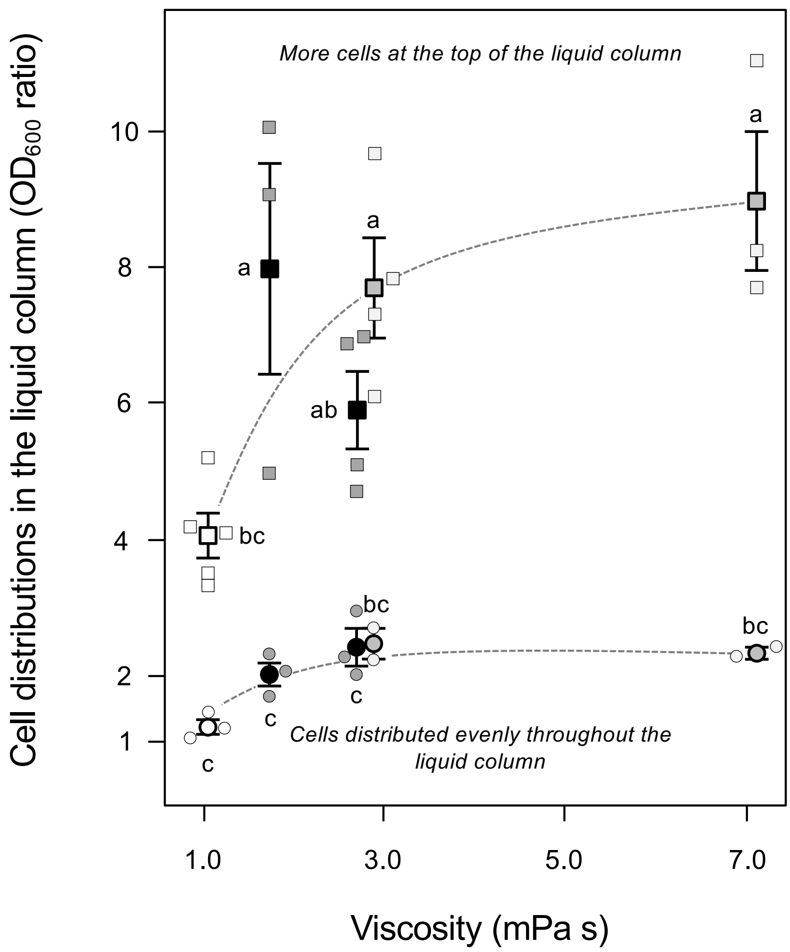

Cell distributions in the liquid column (OD600 ratio)
More cells at the top of the liquid column
Cells distributed evenly throughout the liquid column
a
a
a
ab
bc
bc
bc
c
c
c
10
8
6
4
2
1
1.0
3.0
5.0
7.0
Viscosity (mPa s)

Figure 4

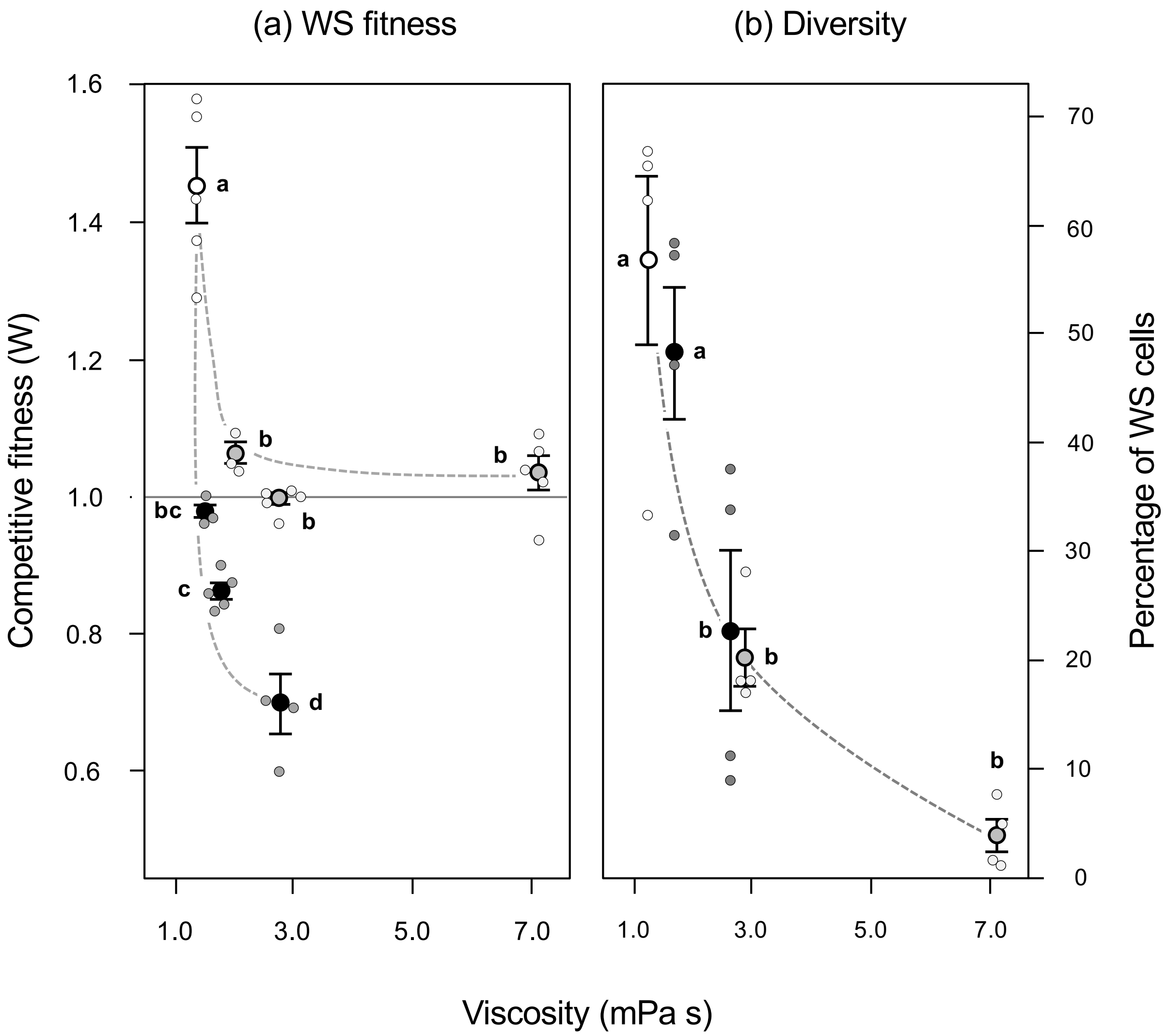

(a) WS fitness
(b) Diversity
Competitive fitness (W)
Percentage of WS cells
Viscosity (mPa s)
1.6
1.4
1.2
1.0
0.8
0.6
70
60
50
40
30
20
10
0
1.0
3.0
5.0
7.0
a
b
bc
c
d

Figure 5

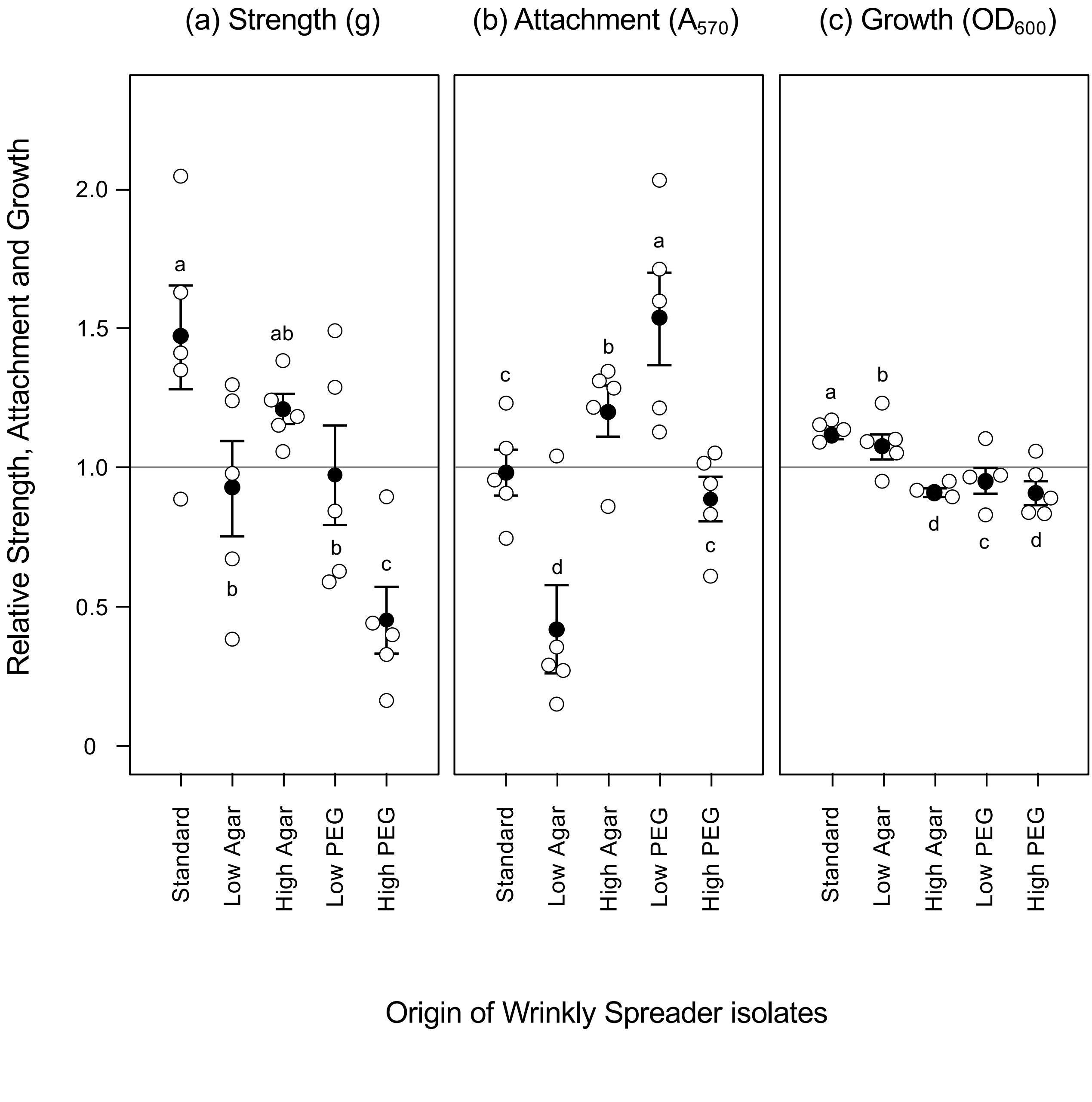
(a) Strength (g)
(b) Attachment (A570)
(c) Growth (OD600)
Relative Strength, Attachment and Growth
2.0
1.5
1.0
0.5
0
a
b
ab
b
c
c
d
b
a
c
a
b
d
c
d
Standard
Low Agar
High Agar
Low PEG
High PEG
Origin of Wrinkly Spreader isolates

Figure 6

Supplementary Information, Table, Figures and References

Penetrating the air-liquid interface is the key to colonization and Wrinkly Spreader fitness

Robyn Jerdan, Anna Kuśmierska, Marija Petric & Andrew J. Spiers

Supplementary Information

Supplementary Information S1. Aerotaxis in soft-agar test tubes.

Test tubes containing soft-agar used to visualise the aerotaxic behaviour of wild-type SBW25 cells. Test tubes were first prepared by setting 5ml soft-agar at the base. A mixture of 500 µl washed cells from an over-night culture and 500 µl soft-agar containing 0.6% (w/v) agar (both equilibriated at 55 °C to prevent setting) was then added and allowed to set at 20 °C. Finally, a further 5 ml soft-agar was added to the top and allowed to set. Ten microliters of 1 mg ml^{-1} tertrazolium violet was added to the cell mixture and 100 µl added to the top of the soft-agar column to track metabolically-active cells. The test tubes were incubated vertically with loose lids for 48 h before inspection.

Supplementary Information S2. Swimming characteristics of strains.

The flagella-mediated swimming motility of wild-type SBW25, the chemotaxic *cheA*$^-$ and flagella-deficient *fleQ*$^-$ mutants have been investigated using soft-agar plate assays and microscopy [1-7], and microscopic observation used to confirm the motility of the Wrinkly Spreader [4] (SBW25 is also capable of twitching and swarming motility [5,7-9]). We have used soft-agar plate assays to confirm the swimming motility of the strains used in this work and observed significant differences in swimming diameters after 24 h (TK-HSD, α = 0.05) (Supplementary Information Figure S2).

Further analysis showed a significant difference in motility between *cheA*$^-$ mutant cells capable of directionless movement and non-motile *fleQ*$^-$ mutant cells (T-test, P = 0.0001). We also note that archetypal WS is less than that of wild-type cells but more than the *cheA*$^-$ and *fleQ*$^-$ mutants (TK-HSD, α = 0.05), suggesting that the expression of cellulose and attachment factor retards movement or increased c-*di*-GMP levels repress flagellum-based motility.

Supplementary Information S3. Diffusivity of non-motile SBW25 cells.

The diffusivity of a non-motile cell is given by the Stokes-Einstein equation for diffusion of spherical particles through a liquid with a low Reynolds number, $[K_B T] / [3 \pi \eta ø]$, where K_B is the Boltzmann constant, T is temperature, η is the dynamic viscosity of the liquid and ø the diameter of the sphere (the Reynolds number is zero as the liquid in static microcosms is at rest). Using our measurements of η for KB (1.26 ± 0.02 mPa s) and a temperature of 20 °C, we estimate D_S as 2.9 – 38 x 10^{-8} μm^2 s^{-1} using the mean SBW25 cell diameter of 0.9 µm and cell body length plus flagella of 11.5 µm from [6] as the spherical diameters.

Supplementary Information S4. Effect of viscosity agents on SBW25.

Modified microcosms used to visually assess the effects of increased viscosity contained a range of additives including agar (Technical No. 3, Oxoid, UK), carboxymethyl cellulose (CMC, Sigma), Ficol 70 (Sigma), and polyethylene glycol (PEG 10,000, Sigma). Microcosms were brought to a brief boil using a microwave oven to melt any gels and then equilibrated at 55 °C before inocula were added, gently mixed and allowed to cool to 20 °C for incubation.

Modified microcosms were inoculated with over-night wild-type SBW25 cultures and growth and cell distributions assessed visually after 24 h (Supplementary Information Table S1). Clear signs of growth were observed in all microcosms, indicating that the brief exposure to 55°C was not lethal nor were the viscosity agents highly toxic.

Supplementary Table S1

Table S1. Effect of viscosity agents on the growth and distribution of *Pf.* SBW25 in static microcosms.

Cause of viscosity	Agent added	Observations
	None	Good growth throughout the liquid column with no visually-obvious localisation at the A-L interface.
Inter-molecular friction	0.3 – 20% Ficol	Good growth throughout the liquid column at 0.6% or lower but localised at the A-L interface at 1.2% or above; poor growth at 20% with solutions becoming very viscous at 10%.
	0.3 – 20% PEG	Good growth throughout the liquid column at 2.5% or lower but localised at the A-L interface at 5% or above; poor growth at 20% with solutions becoming very viscous at 20%.
Inter-molecular network	0.05 – 2% Agar	Good growth throughout the liquid column at 0.05% or lower but localised at the A-L interface at 0.1% or above with gelling at 0.4%.
	0.125 – 1% CMC	Good growth throughout the liquid column at 0.25% or lower but localised at the A-L interface at 0.5% or above with gelling at 1 %.

Observations of static microcosms inoculated with SBW25 were made after 24 hr. CMC, carboxymethyl cellulose; Ficol, Ficol 70; PEG, Polyethylene glycol 10,000; Concentrations are % (w/v).

Supplementary Figures S1 – S4

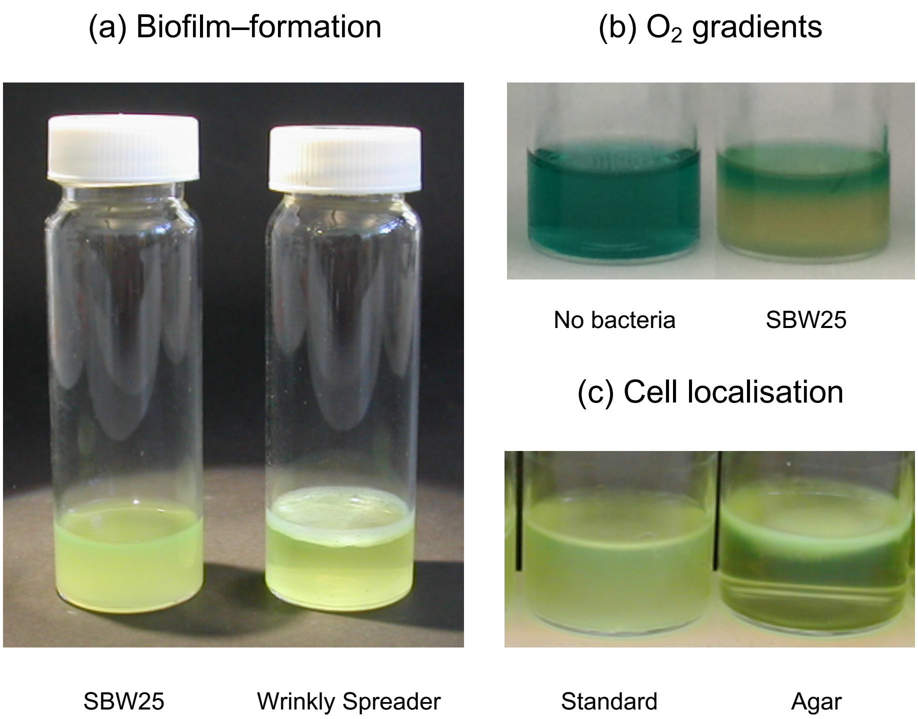

Figure S1. Wrinkly Spreader colonises the A-L interface by biofilm–formation. The Wrinkly Spreader produces a visually-obvious, robust and well-attached biofilm at the A–L interface of static microcosms while under normal conditions wild-type cells grow throughout the liquid column without producing a biofilm (a) (left, Wild-type culture; right, WS culture). The metabolic activity of cells rapidly generates an O_2 gradient down the liquid column leaving a shallow O_2-rich region at the top. This region can be visualised using the O_2-sensitive indicator Methylene blue which is blue/green in the presence of O_2 but is decolourised under low–O_2 conditions (b) (left, Sterile control; right, Wild-type culture). While biofilm–formation is a successful strategy allowing colonization of the A-L interface, increasing liquid viscosity allows wild-type cells to localise at the A-L interface without the need for biofilms (c) (left, standard microcosm; right, modified microcosm with agar).

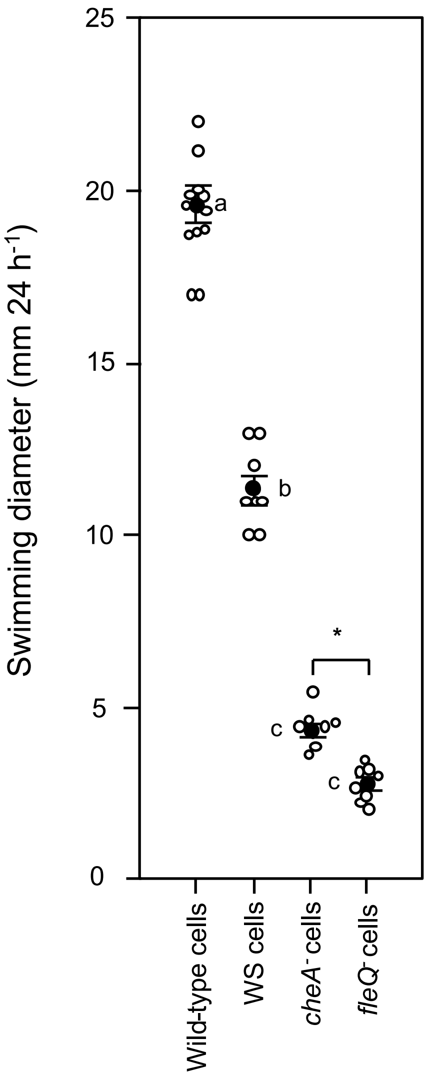

Figure S2. Swimming characteristics of wild-type SBW25 and mutant strains. Soft-agar plates were used to assess flagella-mediated swimming motility (mm 24 h^{-1}). The *fleQ*$^-$ mutant is unable to produce flagella and the mean diameter indicates the effect of random diffusion and growth from the point of inoculation. The *cheA*$^-$ mutant is capable of swimming motility but not chemotaxis, so the diameter indicates non-directed movement and growth out from the point of inoculation. In contrast, wild-type and WS cells are capable of chemotaxis–regulated swimming motility. Means (black circles) ± SE are shown (replicates are indicated by white circles). Means not linked by the same letter are significantly different (TK-HSD, α = 0.05). Further investigation showed a significant difference (*) between *cheA*$^-$ and *fleQ*$^-$ swimming motility (T-test, P = 0.0001).

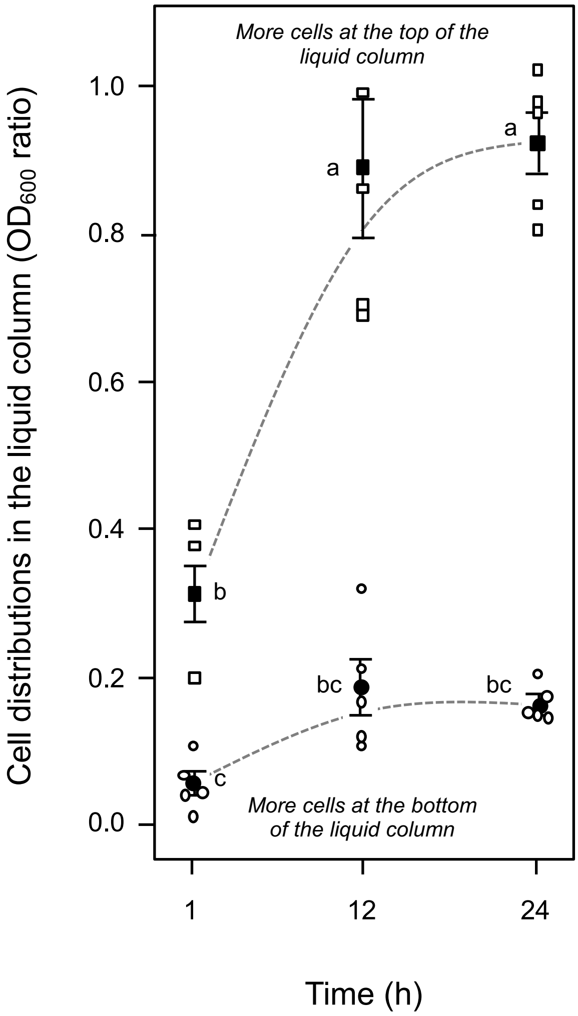

Figure S3. Swimming allows cells to move into the liquid column. Wild-type SBW25 cells (grey squares) are able to migrate from cell pellets placed at the bottom of static microcosms to the top of the liquid column by flagella-mediated swimming within 12 h. In contrast, non-swimming *fleQ*$^-$ mutant cells (black squares) show no significant migration in the same period. Cell distributions were determined from OD_{600} measurements of samples taken from the top and bottom of static microcosms and is shown as the cell distributions in the liquid column (top / bottom OD_{600} ratio). A ratio of one suggests cells are equally distributed throughout the liquid column. Means (black symbols) ± SE are shown (replicates are indicated by white symbols). Means not linked by the same letter are significantly different (TK-HSD, $\alpha = 0.05$) Trend lines (dashed curves) are descriptive only.

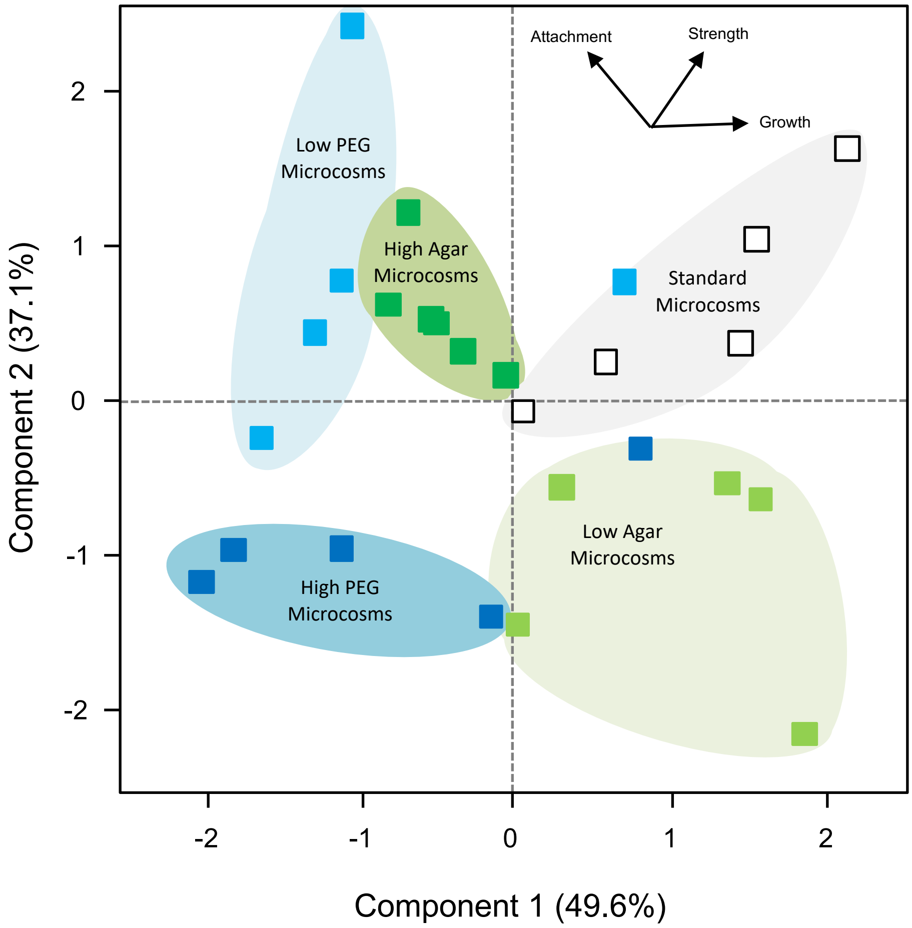

Figure S4. Wrinkly Spreaders isolated from modified microcosms have different biofilm characteristics. Investigation of the combined biofilm mean data (microcosm growth, biofilm strength and attachment levels measured in standard microcosms) examined by PCA could differentiate independent Wrinkly Spreader isolates recovered from standard (white squares), low agar (light green), high agar (dark green), low PEG (light blue) and high PEG (dark blue) microcosms using the first two principle axes (Bartlett tests, *P* = 0.002 and 0.007, respectively). The coloured ovals are suggestive of groupings only. The Eigen vectors for mean biofilm strength (g), attachment levels (A_{570}) and total growth (OD_{600}) are indicated in the top right corner.

Supplementary References

[1] **Bailey MJ, Lilley AK, Thompson IP, Rainey PB, Ellis RJ.** Site directed chromosomal marking of a fluorescent pseudomonad isolated from the phytosphere of sugar beet, stability and potential for marker gene transfer. *Mol Ecol* 1995;4:755–763.

[2] **Turnbull GA, Morgan JAW, Whipps JM, Saunders JR.** The role of bacterial motility in the survival and spread of *Pseudomonas fluorescens* in soil and in the attachment and colonisation of wheat roots. *FEMS Microbiol Ecol* 2001;36:21–31.

[3] **De Weert S, Vermeiren H, Mulders IHM, Kuiper I, Hendrickx N, Bloemberg GV, Vanderleyden J, De Mot R, Lugtenberg BJJ.** Flagella-driven chemotaxis towards exudate components is an important trait for Tomato root colonization by *Pseudomonas fluorescens*. *MPMI* 2002;15:1173–1180.

[4] **Spiers AJ, Rainey PB.** The *Pseudomonas fluorescens* SBW25 wrinkly spreader biofilm requires attachment factor, cellulose fibre and LPS interactions to maintain strength and integrity. *Microbiology* 2005;151:2829–39.

[5] **Jones J, Studholme DJ, Knight CG, Preston GM.** Integrated bioinformatic and phenotypic analysis of RpoN-dependent traits in the plant growth-promoting bacterium *Pseudomonas fluorescens* SBW25. *Environ Microbiol* 2007;9:3046–3064.

[6] **Ping L, Birkenbeil J, Monajembashi S.** Swimming behaviour of the monotrichous bacterium *Pseudomonas fluorescens* SBW25. *FEMS Microbiol Ecol* 2013; 86:36–44.

[7] **Alsohim AS, Taylor TB, Barrett GA, Gallie J, Zhang X-X, Altamirano-Junqueira AE, Johnson, LJ, Rainey PB, Jackson RW.** The biosurfactant viscosin produced by *Pseudomonas fluorescens* SBW25 aids spreading motility and plant growth promotion. *Environ Microbiol* 2014;16:2267–2281.

[8] **Giddens SR, Jackson RW, Moon CD, Jacobs MA, Zhang X-X, Gehrig SM, Rainey PB.** Mutational activation of niche-specific genes provides insight into regulatory networks and bacterial function in a complex environment. *PNAS (USA)* 2007;104:18247–18252.

[9] **Koza A, Hallett PD, Moon CD, Spiers AJ.** Characterisation of a novel air–liquid interface biofilm of *Pseudomonas fluorescens* SBW25. *Microbiol* 2009;155:1397–1406.